Francisco Rouxinol
Instituto de Física Gleb Watghin
Rua Sergio Buarque de Holanda, 777
13083-859, Campinas, SP
e-mail: rouxinol@unicamp.br
tel: +55(19)3521-5462

Grande Área de conhecimento: Ciências Exatas e da Terra
Área de Conhecimento:Física
Subárea de Conhecimento: Física da Matéria Condensada
Aluno(a):Daniel G. Benvenutti RA: 169448
Orientador: Francisco Rouxinol
Instituição: Instituto de Física Gleb Wataghin, UNICAMP
Áreas de enquadramento da proposta: Pesquisa Básica
Áreas de enquadramento CNPq: Tecnologias Habilitadoras: Materiais Avançados e Nanotecnologia
Palavras chaves: Eletrodinâmica Quântica, Informação e Computação Quântica, Circuitos Supercondutores

A study of superconducting circuits for quantum computing

Abstract

The project introduces the student to the hardware of a quantum computer (QCH), more specifically to the hardware based on superconducting circuits based on Josephson junctions. We will study some of the main superconductor circuits used in implementation of QCH like the transmon qubit and the co-planar cavity. using capacitors, inductors and Josephson junctions, we will develop the main elements of these systems, and study the effects that a non-linear component, the Josephson junction, brings them. We will also study the interaction of a microwave cavity with and artificial atom, the transmon, and comprehend how this interaction will alter the states of these systems. using non-Hamiltonian simulations, in the qutip package, we will study the dynamics of this system. At last, we will implement these circuits in the package qiskit metal, an IBM tool, to generate the superconducting quantum circuits using these designs.

Introduction

In MIT's computer physics conference of 1981 Feymann said:[3] " . . . *trying to find a computer simulation of physics seems to me to be an excellent program to follow out. . . . the real use of it would be with quantum mechanics. . . . Nature isn't classical . . . and if you want to make a simulation of Nature, you'd better make it quantum mechanical, and by golly it's a wonderful problem, because it doesn't look so easy*." This citation describes one of the most revolutionary fields of research of modern physics, from computer science and engineering, promising to be able to solve a category of computational problems that a classical computer cannot [8]. The key to

build such device lies in implementing and controlling quantum bits (qubits, a quantum mechanical two level system) in a scalable way. Many approaches were adopted in the creation of different qubit realizations, like Rydberg atoms, electron spins, photons or superconducting circuits based on the Josephson junction [2].

In particular, in the last years there was a great progress in the development of quantum circuits in small scale with many quantum bits (qubits)[1]. However, a quantum computer tolerant to faults that exceeds the development of existing classical machines currently will require a network of thousands or even millions of qubits, much beyond the current technologies [6]. In this manner, the robust knowledge of control techniques and measurement of quantum machines is essential to the understanding of these new technologies. With these words in mind, this project of scientific initiation has as objective the **study of control techniques, measurement of quantum states of a qubit made out of elements of superconducting circuits**. The project will involve the **study of the theory of many devices and fundamental concepts of the quantum technologies, like the simulation and techniques of fabrication of these systems**.

Superconductors: macroscopic quantum phenomena[5]

The macroscopic quantum model

People who are knowledgeable about quantum mechanics know that some quantum phenomena are quantized, manifest in discreet quantities. But it's interesting to notice that this isn't restricted to microscopic phenomena. Thanks to coherence effects the electrons in a superconductor are highly correlated. this can create quantization like in the magnetic flux of a superconducting loop with size orders of magnitude greater than an atom.

Coherent phenomena in superconductivity

The superconducting effect was studied many times by renowned researchers, but it was only really understood when Fritz London realised that it was but a quantum phenomenon manifesting in macroscopic scale.

The macroscopic model of superconductivity assumes that there is a macroscopic wave function $\Psi(\mathbf{r}, t)$ describing the set of electrons. That in turn is justified by the BCS microscopic theory. Based on the idea that electrons feel an attractive force when near the Fermi level. Under a critical temperature the electrons go to a new quantum state where some electrons form Cooper pairs. These pairs don't have angular orbital momentum (estate s) and therefore the Pauli exclusion principle requires that the spins be in a singleto ($||0,0\rangle$). In these pairs case the orbital state radius is much bigger (1nm até 1μm). With a great superposition in between the pairs. The bonding energy between these pairs depends on how many other pairs condensed and the center of mass is highly correlated. So much as that all remain in the same state with the same center of mass of movement.

The wave function of the movement of the mass center can be described as:

$$\Psi(\mathbf{r},t) = \Psi_0 e^{i\theta(\mathbf{r},t)} = \Psi_0 e^{i\mathbf{k}_s\cdot\mathbf{r}-i\omega t} \tag{0.0.1}$$

This is valid for superfluids without charge such as the ^4He, ^3He or the Bose-Einstein condensates.

Finding a quantum equation for electromagnetism

First we need to find **E** and **B** in potential terms. By Gauss's first law we know **B** can be written as:

$$\mathbf{B} = \nabla \times \mathbf{A} \tag{0.0.2}$$

A is a vectorial potential that we can use in the Faraday's law:

$$\nabla \times \mathbf{E} + \frac{\partial \mathbf{B}}{\partial t} = \nabla \times (\mathbf{E} + \frac{\partial \mathbf{A}}{\partial t}) = 0 \tag{0.0.3}$$

That implies:

$$\mathbf{E} = \frac{\partial \mathbf{A}}{\partial t} - \nabla\phi \tag{0.0.4}$$

Because the curl of a gradient of a scalar field ϕ is zero, we get the Lorentz law in the form:

$$m\frac{d\mathbf{v}}{dt} = q[\mathbf{E} + (v \times \mathbf{B})] \tag{0.0.5}$$

Obtained in function of the potentials:

$$m\frac{d\mathbf{v}}{dt} = -q[\nabla\phi + \frac{\partial A}{\partial t} - (\mathbf{v} \times (\nabla \times \mathbf{A}))] \tag{0.0.6}$$

Using the chain rule:

$$\frac{d\mathbf{A}}{dt} = \frac{\partial \mathbf{A}}{\partial t} + (\mathbf{v}\cdot\nabla)\mathbf{A} \tag{0.0.7}$$

We get:

$$\frac{d}{dt}(m\mathbf{v} + q\mathbf{A}) = -q[\nabla\phi + (\mathbf{v}\cdot\nabla)\mathbf{A} - (\mathbf{v} \times (\nabla \times \mathbf{A}))] \tag{0.0.8}$$

We can assume then (proof in reference[5]) that the canonical momentum is $\mathbf{p} = m\mathbf{v}+q\mathbf{A}$, where $m\mathbf{v}$ corresponds to the kinetical momentum and $q\mathbf{A}$ to the field momentum. Then we obtain the law of Lorentz in the general form:

$$\frac{d\mathbf{p}}{dt} = -\nabla\left\{q\phi - \frac{q}{m}(\mathbf{p}\cdot\mathbf{A}) + \frac{q^2}{2m}\mathbf{A}\cdot\mathbf{A})\right\} = -\nabla V \tag{0.0.9}$$

Which shows that the potential isn't a function only of time and space but of the canonical momentum.

To find Schrödinger's equation we need the total energy (to make the hamiltonian):

$$E = E_{kin}+E_{pot} = \frac{\mathbf{p}\cdot\mathbf{p}}{2m}+\left\{q\phi - \frac{q}{m}(\mathbf{p}\cdot\mathbf{A}) + \frac{q^2}{2m}\mathbf{A}\cdot\mathbf{A})\right\} = \frac{1}{2m}(\mathbf{p}-q\mathbf{A})\cdot(\mathbf{p}-q\mathbf{A})+q\phi \tag{0.0.10}$$

Then we substitute the energy and the momentum in the classical equation above (0.0.10)

$$E \rightarrow i\hbar\frac{\partial}{\partial t} \tag{0.0.11}$$

$$\mathbf{p} \rightarrow -i\hbar\nabla \tag{0.0.12}$$

We obtain then the Schrödinger equation for a charged particle in an electromagnetic field:

$$i\hbar\frac{\partial\mathbf{\Psi}}{\partial t} = \frac{1}{2m}\left(\frac{\hbar}{i}\nabla - q\mathbf{A}\right)^2\mathbf{\Psi} + q\phi\mathbf{\Psi} \tag{0.0.13}$$

That has a probability current:

$$\mathbf{J}_\rho = \Re\left\{\Psi^*\left(\frac{\hbar}{m}\nabla - \frac{q}{m}\mathbf{A}\right)\Psi\right\} = \Re\left\{\Psi^*\frac{\hat{\mathbf{p}}}{m}\Psi\right\} \tag{0.0.14}$$

Supercurrent equation:

$$\mathbf{J}_S = q^* n_S^*(\mathbf{r},t)\left\{\frac{\hbar}{m^*}\nabla\theta(\mathbf{r},t) - \frac{q^*}{m^*}\mathbf{A}(\mathbf{r},t)\right\} \tag{0.0.15}$$

Where q^* is the superelectron charge and n_S^* is the electron density (and the content inside the brackets is the speed $\mathbf{v}_s$)

London Equations

They are two equations by Fritz London that describe the behavior of superconductor on the basis of classical physics.

Assuming $n_S^* = cte$ in eq. 0.0.22 (constant electron density).

Using London's coefficient $\Lambda = \frac{m^*}{n_S^* q^{*2}}$ the equation 0.0.22 becomes:

$$\Lambda\mathbf{J}_S = -\left\{\mathbf{A}(\mathbf{r},t) - \frac{\hbar}{q^*}\nabla\theta(\mathbf{r},t)\right\} \tag{0.0.16}$$

Second London equation and the Meissner-Ochsenfeld effect

[h]

With the curl of the expression obtained above we get the second London equation:

$$\nabla\times(\Lambda\mathbf{J}_S) = -\nabla\times\mathbf{A} = -\mathbf{B} \tag{0.0.17}$$

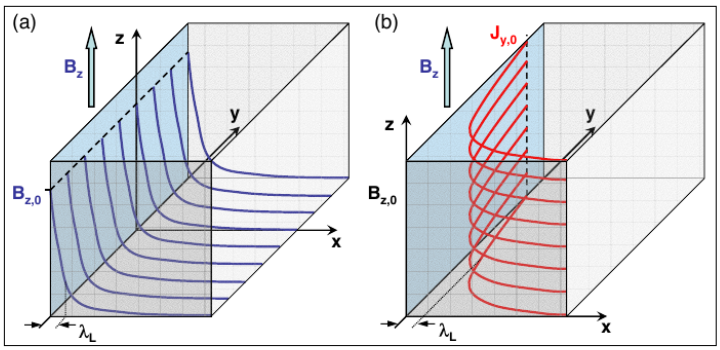

Figure 1.1: Exponential decay of the magnetic field **B** (a) and the supercurrent density $\mathbf{J}_s$ (b) with distance x into a bulk superconductor.

FIGURE 1: Adapted from: [5]

The Meissner-Ochsenfeld effect can be inferred from the equation obtained below: Taking the curl of the Maxwell equation:

$$\nabla \times \nabla \times \mathbf{B} = \nabla \times \mu_0 \mathbf{J}_S \tag{0.0.18}$$

Then the chain rule (left) and the second London equation (right):

$$\nabla(\nabla \cdot B) - \nabla^2 \mathbf{B} = -\frac{\mu_0}{\Lambda}\mathbf{B} \tag{0.0.19}$$

With $\nabla \cdot B = 0$ we get:

$$\nabla^2 \mathbf{B} = \frac{\mu_0}{\Lambda}\mathbf{B} = \frac{1}{\lambda_L^2}\mathbf{B} \tag{0.0.20}$$

Where:

$$\lambda_L \equiv \sqrt{\frac{m^*}{\mu_0 n_S^* q^{*2}}} \tag{0.0.21}$$

This effect shows that we get a exponential decay inside a superconductor with an applied magnetic field where the characteristic decay length is the London penetration depth λ_L.

First London Equation and perfect conductivity

To get the first London equation we take the derivative of eq. 0.0.22

$$\frac{\partial}{\partial t}(\Lambda \mathbf{J}_S) = q^* n_S^*(\mathbf{r}, t) - \left\{ \frac{\partial \mathbf{A}(\mathbf{r}, t)}{\partial t} - \frac{\hbar}{q^*}\nabla \frac{\partial \theta(\mathbf{r}, t)}{\partial t} \right\} \tag{0.0.22}$$

From the equation above, with:

$$-\hbar \frac{\partial \theta}{\partial t} = \frac{1}{2n_S^*}\Lambda \mathbf{J}_S^2 + q^* \phi \tag{0.0.23}$$

And with $\mathbf{E} = -\partial \mathbf{A}/\partial t - \nabla \phi$ we can deduce the first London equation:

$$\frac{\partial}{\partial t}(\Lambda \mathbf{J}_S) = \mathbf{E} - \frac{1}{2n_S^* q^*}\nabla(\frac{1}{2}\Lambda \mathbf{J}_S^2) \tag{0.0.24}$$

The second term in the right side of the London's equation can be neglected (because it's equivalent to the kinetic energy of the superelectrons) so we get:

$$\frac{\partial}{\partial t}(\Lambda \mathbf{J}_S) = \mathbf{E} \tag{0.0.25}$$

Where we can conclude that for a current constant in time the Electric field is zero and therefore we get a dissipation less current. $R = V/I = \int E d\mathbf{r}/I = 0$.

Flux Quantization

Analysis of the quantum mechanical properties of superconductors:

If you take a superconducting ring and apply a stationary current through a magnetic field. It will stay put through the zero resistance property. But it will also assume discreet ie quantized states as a consequence of it's quantumness. As a way that the wave function doesn't interfere destructively with itself. [h] The values of the flux by

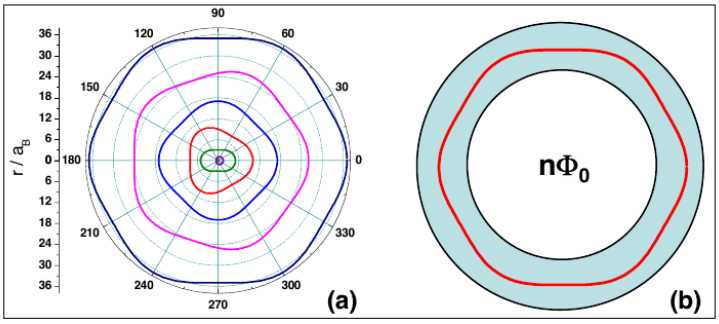

Figure 1.3: Stationary quantum states: (a) The standing electron wave around the nucleus of an atom at $r = 0$ resulting in the Bohr-Sommerfeld quantization of the angular momentum. (b) The standing wave of the macroscopic wave function representing the superconducting state in a superconducting cylinder resulting in flux quantization.

FIGURE 2: Adapted from: [5]

this loop are multiples of the flux quantum:

$$\mathbf{\Phi}_0^L = \frac{h}{e} \approx 4 \times 10^{-15} Vs \tag{0.0.26}$$

But London derived this value without taking into account that the electrons form cooper pairs. We then derive the quantization conditions from the macroscopic models for that we use equation 0.0.16 and integrate in a closed path:

$$\oint (\Lambda \mathbf{J}_S) \cdot d\mathbf{l} = -\oint \mathbf{A} \cdot d\mathbf{l} + \frac{\hbar}{q^*} \oint (\nabla \theta) \cdot d\mathbf{l} \tag{0.0.27}$$

From stokes we get:

$$\oint \mathbf{A} \cdot d\mathbf{l} = \int_S (\nabla \times A) \cdot d\mathbf{s} = \int_S \mathbf{B} \cdot d\mathbf{s} \tag{0.0.28}$$

The closed path integral of a gradient is always zero, but since the phase can actually be written as:

$$\theta(\mathbf{r}, t) = \theta_0(\mathbf{r}, t) + 2\pi n \tag{0.0.29}$$

The result of this path integral is $2\pi n$

Equation 0.0.27 then becomes:

$$\oint (\Lambda \mathbf{J}_S) \cdot d\mathbf{l} + \int_S \mathbf{B} \cdot d\mathbf{s} = \frac{\hbar}{q^*} 2\pi n = \frac{h}{q^*} n = \mathbf{\Phi}_0 n \tag{0.0.30}$$

and:

$$\mathbf{\Phi}_0 = \frac{h}{|q^*|} = \frac{h}{2e} \tag{0.0.31}$$

Consequences:

1. The path defines a simply connected superconducting region: Here we just do the limit of the extremities $r_2 \to r_1$. If the contour line has size zero then we just imply that $n = 0$
2. The path defines a multiply connected superconductor: Because of the hole inside the superconductor when you do the limit $r_1 \to r_2$ they end up having a different phase. Which is $2\pi n$.

Flux and Fluxoid Quantizations

The left side of the 0.0.30 equation is denoted *fluxoid* and so it states the quantization of this fluxoid. Therefore the total flux in a multi-connected superconductor must have discreet values, even with an external magnetic field.

Flux quantization

Assuming we have a superconducting ring with walls much thicker than the penetration depth λ_L and a magnetic field much smaller than the critical field. The magnetic field will pass inside the ring without penetrating the ring itself. On the ring's surface there will be screening supercurrents countering the incoming magnetic field.

In case we cool down the superconductor with a magnetic field applied it can become trapped in it. But respecting the fluxonium quantization conditions though. By choosing somewhere inside the superconductor out of the penetration that where $\mathbf{J}_S \approx 0$ we get:

$$\int_S \mathbf{B} \cdot d\mathbf{s} = n\Phi_0 \tag{0.0.32}$$

Which implies that quantization condition mentioned earlier.

Flux Trapping

From the first London equation with $\partial \mathbf{J}_S / \partial t = 0$, $\mathbf{E} = \partial \mathbf{A}/\partial t - \nabla\phi$ and $\nabla\phi = 0$ we get:

$$\oint \mathbf{E} \cdot d\mathbf{l} = \frac{\partial}{\partial t} \oint \mathbf{A} \cdot d\mathbf{l} = -\frac{\partial}{\partial t} \int_S \mathbf{B} \cdot d\mathbf{s} = -\frac{\partial \phi}{\partial t} \tag{0.0.33}$$

Taking the path inside the superconductor so that $\mathbf{E} = 0$ we get $\partial\phi/\partial t = 0$. Which means the flux inside the cylinder. stays constant. The supercurrents adjust themselves to maintain that.

Josephson Effect

This effect is observed if two superconductors are weakly connected by an electrical contact. Which can be a tunneling barriers, point contacts or regular conducting layers connecting them.

The initial work by Josephson was SIS (superconductor insulator superconductor). For regular metals it's known that some electrons tunnel through the barrier with rate decaying exponentially to the length of the barrier. For superconductors there aren't regular electrons at Fermi level. So there will be *no* tunneling unless we get a voltage smaller than twice the energy gap voltage $V < 2\Delta/e$. For a greater voltage the Cooper pairs can be broken and then tunnel through the barrier.

About the possibility of a whole cooper pair tunneling. The probability is expected to be the square of the probability of a single electron $p_t \leq 10^{-4}$ so p_t^2. Though Brian Josephson discovered that the probability is the same for a single electron. Because the tunneling of the pairs is coherent.

Also there is the **Josephson coupling energy** that works similar to the binding energy of a molecule. Because like the wave functions of the electrons of a hydrogen molecule overlap so does the wave functions of the two superconductors.

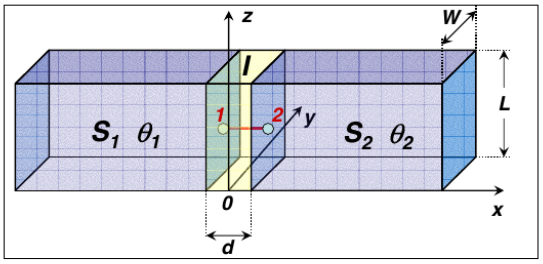

Figure 1.11: Sketch of a superconductor-insulator-superconductor (SIS) Josephson junction with a current source driving a current through the junction.

FIGURE 3: Adapted from: [5]

[h]

The Josephson Equations

First Josephson Equation: current-phase relation

We first assume that the supercurrent in the barrier is not great enough to affect $|\Psi|^2$ of either junction. Which is proportional to the cooper pair densities. However we expect the phase difference to play a role instead.

The supercurrent depends on the gauge invariant phase gradient:

$$J_s(\mathbf{r},t) = \frac{q^* n_s^* \hbar}{m^*}\left[\nabla\theta(\mathbf{r},t) - \frac{2\pi}{\Phi_0}\mathbf{A}(\mathbf{r},t)\right] = \frac{q^* n_s^* \hbar}{m^*}\gamma(\mathbf{r},t) \tag{0.0.34}$$

To simplify we assume:

I The current density is homogeneous

II The phase gradient γ is varying negligibly in the electrodes

III $\mathbf{J}_s$ is the same in the electrodes and the junction area (current conservation)

Since γ is invariant outside the junction region. For that reason we use the **gauge-invariant phase difference** ϕ:

$$\phi(\mathbf{r},t) = \int_1^2 \gamma(\mathbf{r},t) = \int_1^2 \left(\nabla\theta - \frac{2\pi}{\Phi_0}\mathbf{A}\right)\cdot d\mathbf{l} = \theta_2(\mathbf{r},t) - \theta_1(\mathbf{r},t) + \int_1^2 \frac{2\pi}{\Phi_0}\mathbf{A}(\mathbf{r},t)\cdot d\mathbf{l} \tag{0.0.35}$$

With an integration path along the current. That is, across the barrier from the superconductor with phase θ_1 to θ_2. And in the barrier.

$\mathbf{J}_s$ is a function only of ϕ thus $\mathbf{J}_s(\phi)$. But since the change of phase in a wave function is periodic. The current is also periodic in relation to the phase difference.

$$\mathbf{J}_s(\phi) = \mathbf{J}_s(\phi + n2\pi) \tag{0.0.36}$$

Also in case $\theta_1 = \theta_2$ we get a zero current $\mathbf{J}_S(0 + 2n\pi) = 0$

General case supercurrent on josephson junction:

$$\mathbf{J}_S(\phi) = \mathbf{J}_C \sin\phi + \sum_{m=2} \mathbf{J}_m \sin(m\phi) \approx \mathbf{J}_C \sin(\phi) \tag{0.0.37}$$

$\mathbf{J}_c$ is the critical or maximum Josephson current density determined by the coupling strength. The second term can be neglected in most cases.

The essence of this last equation can be summarized as:

The supercurrent density through a Josephson junction varies with the sine of the phase difference across the junction in the absence of scalar and vector potentials

Second Josephson Equation

We derivate the gauge invariant phase different:

$$\frac{\partial\phi}{\partial t} = \frac{\partial\theta_1}{\partial t} + \frac{\partial\theta_2}{\partial t} - \frac{2\pi}{\Phi_0}\frac{\partial}{\partial t}\int_1^2 \mathbf{A}(\mathbf{r},t)\cdot d\mathbf{l} \tag{0.0.38}$$

Energy-phase relation:

$$-\hbar\frac{\partial\theta}{\partial t} = \frac{1}{2n_s^*}\Lambda\mathbf{J}_S^2 + q^*\phi \tag{0.0.39}$$

Substituting 0.0.39 into 0.0.40:

$$\frac{\partial\phi}{\partial t} = \frac{1}{\hbar}\left(\frac{1}{2n_s^*}\Lambda(\mathbf{J}_S^2(2) - \mathbf{J}_S^2(1)) + q^*(\phi(2) - \phi(1))\right) - \frac{2\pi}{\Phi_0}\frac{\partial}{\partial t}\int_1^2 \mathbf{A}(\mathbf{r},t)\cdot d\mathbf{l} \tag{0.0.40}$$

We can assume $\mathbf{J}_S(2) = \mathbf{J}_S(1)$ because the current across the junction is continuous. Also $q^*/\hbar = 2\pi/\Phi_0$ resulting:

$$\frac{\partial\phi}{\partial t} = \frac{2\pi}{\Phi_0}\int_1^2 -\left(\nabla\phi + \frac{\partial\mathbf{A}}{\partial t}\right)\cdot d\mathbf{l} = \frac{2\pi}{\Phi_0}\int_1^2 \mathbf{E}(\mathbf{r},t)\cdot d\mathbf{l} \tag{0.0.41}$$

Which is the second Josephson equation. The integral is just the potential difference V between the two superconductors

With a constant voltage V we get:

$$\phi(t) = \phi_0 + \frac{2\pi}{\Phi_0} Vt \tag{0.0.42}$$

And we get a Josephson current:

$$I_S(t) = I_C \sin \phi(t) \tag{0.0.43}$$

The Josephson frequency is given by $\frac{\nu}{V}$:

$$\frac{\nu}{V} = \frac{\frac{V}{\Phi_0}}{V} = \frac{1}{\Phi_0} \approx 483.6 \frac{MHz}{\mu V} \tag{0.0.44}$$

We can see by this that the Josephson junction is an oscillator controlled by voltage that can generate very high frequencies with a high sensitivity to the voltage input.

Josephson Tunneling

Now we use the wave matching method to find the maximum Josephson current density $\mathbf{J}_C$ on a tunneling barrier of thickness d. We will solve the Schrödinger equation for each superconductor electrode and the barrier and then match the solutions at the boundaries to determine the missing coefficients. The wave function for the electrodes is given by:

$$J_s(\mathbf{r}, t) = q^* n_S(\mathbf{r}, t) \left[\frac{\hbar}{m^*} \nabla\theta(\mathbf{r}, t) - \frac{q^*}{m^*} \mathbf{A}(\mathbf{r}, t) \right] \tag{0.0.45}$$

The relationship between the current density and the phase is given by 0.0.37, the current-phase relation. We then assume a uniform tunneling barrier and that the junction $Area = Length \cdot Width$ is small enough for the current density to be assumed uniform in the junction area (constant on y and Z). Approximating the energy-phase relation 0.0.23:

$$-\hbar \frac{\partial \theta}{\partial t} = \frac{1}{2n_S^*} \Lambda \mathbf{J}_S^2 \tag{0.0.46}$$

The term on the right hand corresponds to the kinetic energy of the superelectrons, so we write:

$$-\hbar \frac{\partial \theta}{\partial t} = -\frac{E_0}{\hbar} \tag{0.0.47}$$

And the time dependent wave function is thus:

$$\Psi(\mathbf{r}, t) = \Psi(\mathbf{r}) e^{-i(E_0/\hbar)t} \tag{0.0.48}$$

Now to determine the wave function on the insulating barrier. The height of the potential of the barrier V_0 is assumed greater than E_0. Therefore the potential function $V(x)$ is a rectangular function with height V_0 and thickness d. We assume that the process is elastic (the superelectrons maintain their energy) so the time evolution is the same inside and outside the barrier. The Schrödinger equation is then:

$$-\frac{\hbar^2}{2m^*}\nabla^2\Psi(\mathbf{r}) = (E_0 - V_0)\Psi(\mathbf{r}) \tag{0.0.49}$$

Which is time independent because the potential V_0 is a constant. The solution is a simple sum of decaying and increasing exponentials:

$$\Psi(x) = A\cosh(\kappa x) + B\sinh(\kappa x) \tag{0.0.50}$$

$$\kappa = \sqrt{\frac{2m^*(V_0 - E_0)}{\hbar^2}} \tag{0.0.51}$$

The boundaries at $\pm d/2$ give:

$$\Psi(-d/2) = \sqrt{n_1^*}e^{i\theta_1} \tag{0.0.52}$$

$$\Psi(+d/2) = \sqrt{n_2^*}e^{i\theta_2} \tag{0.0.53}$$

Solving these with 0.0.50 we get:

$$A = \frac{\sqrt{n_1^*}e^{i\theta_1} + \sqrt{n_2^*}e^{i\theta_2}}{2\cosh(\kappa d/2} \tag{0.0.54}$$

$$B = \frac{\sqrt{n_1^*}e^{i\theta_1} - \sqrt{n_2^*}e^{i\theta_2}}{2\sinh(\kappa d/2} \tag{0.0.55}$$

With the supercurrent density:

$$\mathbf{J}_S = \frac{q^*}{m^*}\Re\left\{\Psi^*\left(\frac{\hbar}{i}\nabla\right)\Psi\right\} \tag{0.0.56}$$

And substituting 0.0.50 we get now:

$$\mathbf{J}_S = \frac{q^*}{m^*}\kappa\hbar\Re\{A^*B\} \tag{0.0.57}$$

Substituting A and B will wield the supercurrent density equation 0.0.37 ($\phi = \theta_2 - \theta_2$) and the maximum Josephson current density will be:

$$\mathbf{J}_C = -\frac{q^*}{m^*}\kappa\hbar\frac{\sqrt{n_1^*n_2^*}}{2\sinh(\kappa d/2)\cosh(\kappa d/2)} = -\frac{q^*\kappa\hbar}{m^*}\frac{\sqrt{n_1^*n_2^*}}{\sinh(\kappa d)} \tag{0.0.58}$$

In practice the barrier height V_0 is of the order of a few eV and thus the decay $1/\kappa$ is less than a nanometer. The thickness of the barrier is a few nanometers therefore $\kappa d \gg 1$. In this case we can approximate $\sinh(2\kappa d)$ to $\frac{1}{2}e^{2\kappa d}$. Getting:

$$\mathbf{J}_C = -\frac{q^*\kappa\hbar}{m^*}2\sqrt{n_1^*n_2^*}e^{-2\kappa d} \tag{0.0.59}$$

[h]

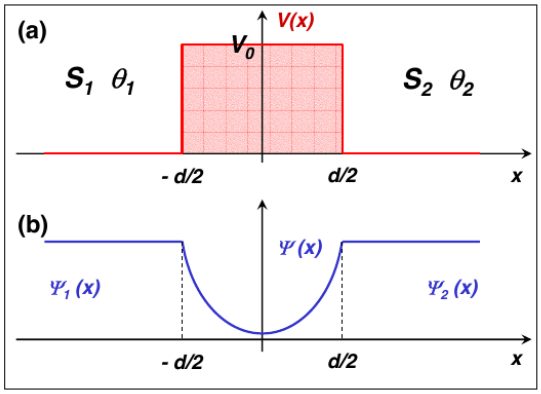

Figure 1.12: (a) Sketch of the model potential $V(x)$ of a superconductor-insulator-superconductor Josephson junction. (b) Time independent part of the wave function.

FIGURE 4: Adapted from: [5]

Circuit QED: Superconducting Qubits coupled to microwave photons[4]

Quantum Electrical Circuits

Quantum LC oscillator

A LC oscillator is composed of a capacitor and a inductor that oscillates just like a mass spring oscillator. With the charge accumulating on the capacitor and stopping current flow and then the flow starting again and accumulating flux on the inductor. Given that the the supercurrent can flow without dissipation and the Coulomb interaction lifts the density fluctuations to optical frequencies we can approximate the LC oscilator as having a single degree of freedom of low energy. The uniform current flow on the inductor wire which builds charge only on the capacitor. This works well on a limit where the size of the wire is much smaller than the wavelength of light at the frequency of oscillation.

[h]

The Lagrangian of the system is:

$$\mathcal{L} = \frac{1}{2}LI^2 - \frac{1}{2}\frac{q^2}{C} \tag{0.0.60}$$

The current is $I = \dot{q}$ and the momentum conjugate is the flux:

$$\frac{\partial \mathcal{L}}{\partial \dot{q}} = L\dot{q} = LI = \Phi \tag{0.0.61}$$

Thus the Hamiltonian is:

$$H = \Phi\dot{q} - \mathcal{L} = \frac{\Phi^2}{2L} + \frac{1}{2C}q^2 \tag{0.0.62}$$

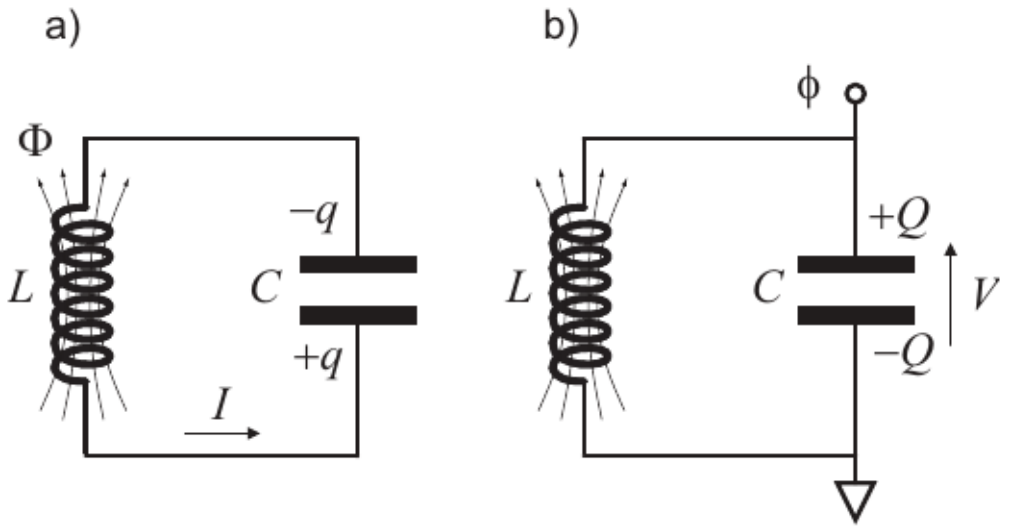

Fig. 2.2 Simple LC electrical oscillator analogous to a mass and spring mechanical oscillator. In panel a) the position coordinate of the mass is taken to be q, the charge accumulated on the capacitor by the current I flowing through the inductor, and the flux Φ through the inductor is the momentum. The sign convention for the charge is such that $\dot{q} = I$ and therefore the inductance L is analogous to the mass. The role of the spring constant is played by $1/C$ and the potential energy of the capacitor is $(q - q_q)^2/2C$, where q_0 is the offset charge of the capacitor (the equivalent of the equilibrium length of the spring). Hamilton's equation for the time rate of change of the momentum is $\dot{\Phi} = -(q - q_0)/C$. In panel b) the position coordinate is now taken to be ϕ, the time integral of the voltage V across the capacitor (i.e., the node flux) and the conjugate momentum is Q, the charge on the capacitor resulting from the electrochemical potential difference between the two plates. The role of the mass is played by C and the spring constant is now $1/L$, with the energy of the inductor given by $(\phi - \phi_0)^2/2L$, where ϕ_0 is the external flux in the loop of the circuit (including the coil of the inductor). Hamilton's equation for the time rate of change of position is $\dot{\phi} = Q/C$. Note the important sign change in the denition of charge: $Q = q_0 - q$, needed to make the Hamilton equations of motion correct in each case. The classical Poisson brackets and the quantum canonical commutation relations between position and momentum are maintained between the two cases: $[\hat{q}, \hat{\Phi}] = [\hat{\phi}, Q] = +i\hbar$.

FIGURE 5: Adapted from: [4]

The voltage on the capacitor is just $V = \dot{\Phi}$.

Quantizing the system we will get the non commuting opperators:

$$[\hat{\Phi}, \hat{q}] = -i\hbar \tag{0.0.63}$$

And the Hamiltonian can be written just like a regular harmonic oscillator:

$$H = \hbar\frac{1}{\sqrt{LC}}(a^\dagger a + \frac{1}{2}) = \hbar\omega(a^\dagger a + \frac{1}{2}) \tag{0.0.64}$$

And we can use the operators a and $a^\dagger$ the same way as a regular Quantum Harmonic

Oscillator. With the capacitance as the inverse of the spring constant $C = \frac{1}{k}$ and the inductance as the mass $L = m$.

Fig. 2.3 LC oscillator wave function amplitude (left panel) and probability density (right panel) plotted vs. the coordinate ϕ. Solid: ground state, Ψ_0; Long-Dashed: first excited state, Ψ_1; Short-dashed: linear combination of the ground and first excited states, $\frac{1}{\sqrt{2}}(\Psi_0 + \psi_1)$.

FIGURE 6: Adapted from: [4]

[h]

Since we will use nonlinear inductors later it's more convenient to use the node flux:

$$\Phi(t) = \int^t d\tau V(\tau) \tag{0.0.65}$$

Which implies $V(t) = \dot{\Phi}(t)$.

The potential and kinetic energy will be respectively:

$$U = \frac{1}{2}C\dot{\Phi}^2 \tag{0.0.66}$$

$$T = \frac{1}{2L}\Phi^2 \tag{0.0.67}$$

Also the Hamiltonian can be written as:

$$H = \hbar\omega(a^\dagger a + \frac{1}{2}) \tag{0.0.68}$$

Just like the QHO. The charge and flux operators are:

$$\hat{Q} = -iQ_{ZPF}(a - a\dagger) = -i\sqrt{\frac{\hbar}{2Z}}(a - a\dagger) \tag{0.0.69}$$

$$\hat{\phi} = \Phi_{ZPF}(a + a^\dagger) = \sqrt{\frac{\hbar Z}{2}}(a + a^\dagger) \tag{0.0.70}$$

$Z = \sqrt{\frac{L}{C}}$ is the characteristic impedance of the oscillator. And using the superconducting resistance quantum:

$$R_Q = \frac{h}{(2e)^2} \approx 6453.20\Omega \tag{0.0.71}$$

we get a dimensionless characteristic impedance:

$$z = Z/R_Q \tag{0.0.72}$$

The characteristic charge and flux are thus:

$$Q_{ZPF} = \sqrt{\frac{C\hbar\omega}{2}} = \sqrt{\frac{\hbar}{2Z}} = 2e\sqrt{\frac{1}{4\pi z}} \tag{0.0.73}$$

$$\Phi_{ZPF} = \sqrt{\frac{L\hbar\omega}{2}} = \sqrt{\frac{\hbar Z}{2}} = \frac{h}{2e}\sqrt{\frac{z}{4\pi}} \tag{0.0.74}$$

Where the uncertainty product is obeyed:

$$Q_{ZPF}\Phi_{ZPF} = \frac{\hbar}{2} \tag{0.0.75}$$

The superconducting flux quantum above is given by

$$\Phi_0 = \frac{h}{2e} \approx 2.06783367\mu V/GHz \tag{0.0.76}$$

Which tells us that that the vacuum fluctuation of the voltage across a capacitor with 10GHz and $Z = 100\Omega$ impedance in the resonator circuit is on the scale of $0.333\mu V$ which is interesting for being in the same scale of the routinely measured audio range.

Driven LC Oscillators

To drive an LC oscillator we need to use a current source ideally. Because a voltage source has zero impedance and would interrupt the oscillation (cause damping). In practice you use a resonator that will be driven by a capacitor or antenna that introduces a bit of damping.

[h]

The drive Lagrangian for the classical circuit would be:

$$\mathcal{L} = \frac{1}{2}C\dot{\phi}^2 - \frac{1}{2L}\phi^2 + I_b(t)\phi \tag{0.0.77}$$

The hamiltonian is:

$$H = \frac{Q^2}{2C} + \frac{\phi^2}{2L} - I_b(t)\phi \tag{0.0.78}$$

You can also use a voltage source. But it has to be in series with the capacitor and inductor.

Coherent States

We obtain a coherent state by driving a quantum system with a external classical force so that the ground state is mapped to it.

$$\Psi_0(\phi) \rightarrow \Psi_\Delta(\phi) = \Psi_0(\phi - \Delta) \tag{0.0.79}$$

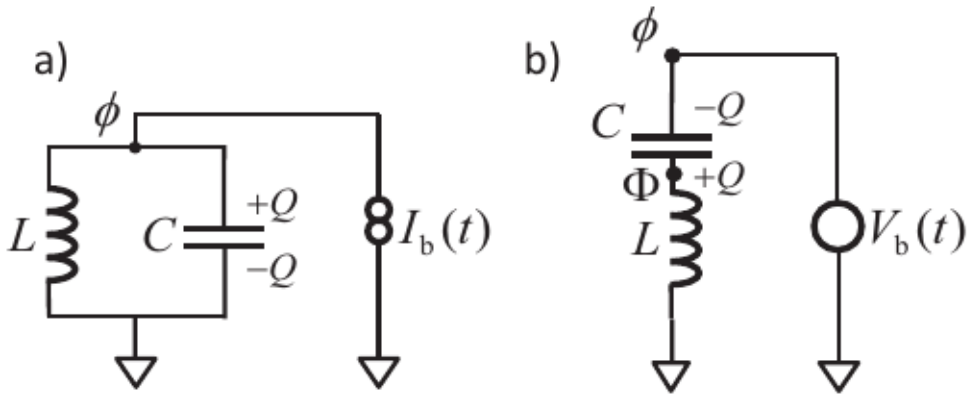

Fig. 2.4 (a) Parallel LC oscillator driven at the node ϕ by a classical external current source with infinite impedance. (b) Series LC oscillator driven at the node ϕ by a classical external voltage source with zero impedance.

FIGURE 7: Adapted from: [4]

You can also displace a coherent state in momentum (charge). It can be written too as:

$$\Psi_\Delta(\phi) = e^{-\Delta\frac{\partial}{\partial\phi}}\Psi_0(\phi) = e^{-\frac{i}{\hbar}\Delta\hat{Q}}\Psi_0(\phi) = e^{-\alpha(a-a^\dagger)}\Psi_0(\phi) = U_\alpha\Psi_0(\phi) \tag{0.0.80}$$

Where $\alpha = \Delta Q_{ZPF}/\hbar = \Delta 2\Phi_{ZPF}$

The state is thus using the Feynman disentangling theorem:

$$|\alpha\rangle = e^{-\frac{1}{2}|\alpha|^2}e^{\alpha a^\dagger}|0\rangle \tag{0.0.81}$$

The coherent state has the following properties:

$$a|\alpha\rangle = \alpha|\alpha\rangle \tag{0.0.82}$$

But it's not an eigenstate of $a^\dagger$. The mean photon number is:

$$\langle\alpha|N|\alpha\rangle = |\alpha|^2 = \bar{N} \tag{0.0.83}$$

The phonon number distribuition is a Poisson:

$$P_n = |\langle n|\alpha\rangle|^2 = \frac{\bar{N}}{n!}e^{-\bar{N}} \tag{0.0.84}$$

Time evolution:

$$|\alpha(t)\rangle = |e^{-i\omega t}\alpha(0)\rangle = e^{\frac{1}{2}|\alpha|^2}e^{\alpha e^{-i\omega t}a^\dagger}|0\rangle \tag{0.0.85}$$

This corresponds to a circular motion in phase space of the simple harmonic oscillator.

$$\hat{X} = \frac{1}{2}[a + a^\dagger] \tag{0.0.86}$$

$$\hat{Y} = -i\frac{1}{2}[a - a^{\dagger}] \tag{0.0.87}$$

$$[X, Y] = \frac{i}{2} \tag{0.0.88}$$

$$\langle\alpha|X|\alpha\rangle = \text{Real}\{\alpha(t)\} \tag{0.0.89}$$

$$\langle\alpha|Y|\alpha\rangle = \text{Imaginary}\{\alpha(t)\} \tag{0.0.90}$$

$$\epsilon = X^2 + Y^2 = N + \frac{1}{2} \tag{0.0.91}$$

A coherent state is nothing more than a displaced vacuum state:

$$|\alpha\rangle = U_{\alpha}|0\rangle \tag{0.0.92}$$

Where α is the classical amplitude of the motion and if $|\alpha| \gg 1$ it dominates over the quantum fluctuations around the classical value. The α value is much greater compared to the deviation of the distribuition.

Writing the X quadrature amplitude as:

$$X = \alpha + \Delta X \tag{0.0.93}$$

The standard deviation operator above has the same properties as the sd of the position in vacuum state.

The number fluctuation is given bellow:

$$\langle\alpha|\Delta N^2|\alpha\rangle = \langle\alpha|[2\alpha\Delta X + \Delta X^2 + \Delta Y^2 - 1/2]^2|\alpha\rangle = \bar{N} \tag{0.0.94}$$

This means a coherent laser or beam is as classical as possible.

Fluctuations in the quadrature orthogonal to α cause uncertainty in a measurement of the coherent state. If $\alpha \in \mathbb{R}$ and $|\alpha| \gg 1$.

$$\Delta \approx \frac{\Delta Y}{\alpha} \tag{0.0.95}$$

$$\langle\alpha(\Delta\theta)^2|\alpha\rangle = \frac{1}{4N} \tag{0.0.96}$$

Thus we arrive at the fundamental number-phase uncertainty:

$$\sqrt{\langle\alpha|\Delta\theta^2|\alpha\rangle}\sqrt{\langle\alpha|\Delta N^2|\alpha\rangle} \geq \frac{1}{2} \tag{0.0.97}$$

From the equation of motion of the free oscillator we see that the quadrature of the amplitudes obey:

$$X(t) = \cos(\omega t)X(0) + \sin(\omega t)Y(0) \tag{0.0.98}$$

$$X(t) = \cos(\omega t)Y(0) - \sin(\omega t)X(0) \tag{0.0.99}$$

The sin and cos parts are quadrature of a quantum electrical signal and are canonically conjugate and thus can't be measured with perfect accuracy.

Coupled LC Resonators

Now we will quantize a pair of LC oscillators coupled by a capacitor. The Lagrangian will be:

$$\mathcal{L} = \frac{1}{2}C_1\dot{\Phi}_1^2 + \frac{1}{2}C_2\dot{\Phi}_2^2 + \frac{1}{2}C_0[\dot{\Phi}_1 - \dot{\Phi}_2]^2 - \frac{1}{2L_1}\Phi_1^2 - \frac{1}{2L_2}\Phi_2^2 \tag{0.0.100}$$

In matrix notation:

$$\mathcal{L} = \frac{1}{2}\dot{\Phi}\mathbf{C}\dot{\Phi} - \frac{1}{2}\Phi\mathbf{L}^{-1}\Phi \tag{0.0.101}$$

$$\mathbf{C} = \begin{pmatrix} C_1 + C_0 & -C_0 \\ -C_0 & C_2 + C_0 \end{pmatrix} \tag{0.0.102}$$

$$\mathbf{L}^{-1} = \begin{pmatrix} 1/L_1 & 0 \\ 0 & 1/L_2 \end{pmatrix} \tag{0.0.103}$$

Method I: Find the hamiltonian then diagonalize

Canonical momenta:

$$Q_i = \frac{\delta\mathcal{L}}{\delta\dot{\Phi}_i} = C_{ij}\dot{\Phi}_j \tag{0.0.104}$$

With the Eistein notation for repeated indices.

The canonical momenta in terms of the inverse capacitance matrix:

$$\dot{\Phi} = C^{-1}Q \tag{0.0.105}$$

The Hamiltonian in the canonical form is now:

$$H = \frac{1}{2}QC^{-1}Q + \frac{1}{2}\Phi L^{-1}\Phi \tag{0.0.106}$$

$$C^{-1} = \frac{1}{C_1C_2 + C_0C_2 + C_0C_2}\begin{pmatrix} C_2 + C_0 & C_0 \\ C_0 & C_1 + C_0 \end{pmatrix}$$

(0.0.107)

We now define two frequencies and a coupling constant:

$$\omega_l^2 = \frac{1}{L_j}(C^{-1})_{jj} \tag{0.0.108}$$

$$\beta = \frac{C_0}{\sqrt{(C_1 + C_0)(C_2 + C_0)}} \tag{0.0.109}$$

Then the inverse capacitance matrix becomes:

$$C^{-1} = \begin{pmatrix} L_1\omega_1^2 & \beta\sqrt{L_1L_2}\omega_1\omega_2 \\ \beta\sqrt{L_1L_2}\omega_1\omega_2 & L_2\omega_2 \end{pmatrix} \tag{0.0.110}$$

We can now write the Hamiltonian $H = H_0 + V$ in terms of two oscillators with masses L_j coupled through their momenta.

$$H_0 = \frac{1}{2}L_1\omega_1^2Q_1^2 + \frac{1}{2L_1}\Phi_1^2 + \frac{1}{2}L_2\omega_2^2Q_2^2 + \frac{1}{2L_2}\Phi_2^2 \tag{0.0.111}$$

$$V = \beta\sqrt{L_1L_2}\omega_1\omega_2Q_1Q_2 \tag{0.0.112}$$

The quantization renders the canonical commutation relation:

$$[\hat{Q}_i, \hat{\Phi}_j] = i\hbar\delta_{ij} \tag{0.0.113}$$

Finally we get with the anihilation creation operators:

$$H_0 = \sum_{j=0}^{2} \hbar\omega_j \left(\hat{a}_j^\dagger\hat{a}_j + \frac{1}{2}\right) \tag{0.0.114}$$

$$V = -\beta\hbar\sqrt{\omega_1\omega_2})(\hat{a}_1 - \hat{a}_1^\dagger)(\hat{a}_2 - \hat{a}_2^\dagger) \tag{0.0.115}$$

Which can be diagonalized with the Bogoljubov transformation.

Method II: Diagonalize the lagrangian, then the hamiltonian:

The first method used the original coordinates and found thier canonical momenta and from there constructed the non-diagonal Hamiltonian. Here we will find the normal mode coordinates which diagonalize the Lagrangian. In terms of these, the Hamiltonian will be automatically diagonal.

But the capacitance and inductance matrices do not commute. To solve that problem we make a similiarity transformation which maps L^-1 to the identity matrix. We then choose scaled coordinates:

$$\psi_j = \frac{1}{\sqrt{L_j}}\Phi_j \tag{0.0.116}$$

The Lagrangian now:

$$\mathcal{L} = \frac{1}{2}\dot{\psi}_iA_{ij}\dot{\psi}_j - \frac{1}{2}\psi_i\delta_{ij}\psi_j \tag{0.0.117}$$

Where:

$$A = \begin{pmatrix} \frac{1}{\Omega_1^2} & -\frac{\beta}{\Omega_1\Omega_2} \\ -\frac{\beta}{\Omega_1\Omega_2} & \frac{1}{\Omega_2^2} \end{pmatrix} \tag{0.0.118}$$

And:

$$\Omega_1^2 = \frac{1}{L_1(C_1 + C_2)} \tag{0.0.119}$$

$$\Omega_2^2 = \frac{1}{L_2(C_2 + C_0)} \tag{0.0.120}$$

Letting S be the transformation matrix that diagonalizes A the normal modes and eigenvalues are then:

$$\tilde{\psi} = S\psi \tag{0.0.121}$$

$$\tilde{A} = SAS^T = \begin{pmatrix} \frac{1}{\Omega_1^2} & 0 \\ 0 & \frac{1}{\Omega_2^2} \end{pmatrix} \tag{0.0.122}$$

Modes of Transmission Lines Resonators

The topic of transmission lines will start with finite length transmission lines. That have discrete electromagnetic resonances, each an independent simple harmonic oscillator. Then we will move to the semi-infinite ones. And see that they can act as a dissipative bath even without dissipative elements. Our finite length line can be a coaxial cable or that which is relevant to the subject a 2D coplanar waveguide (CPW). Which is nothing but superconducting wire evaporated on an insulating substrate and with adjacent superconducting ground planes on the same surface. Figure 8

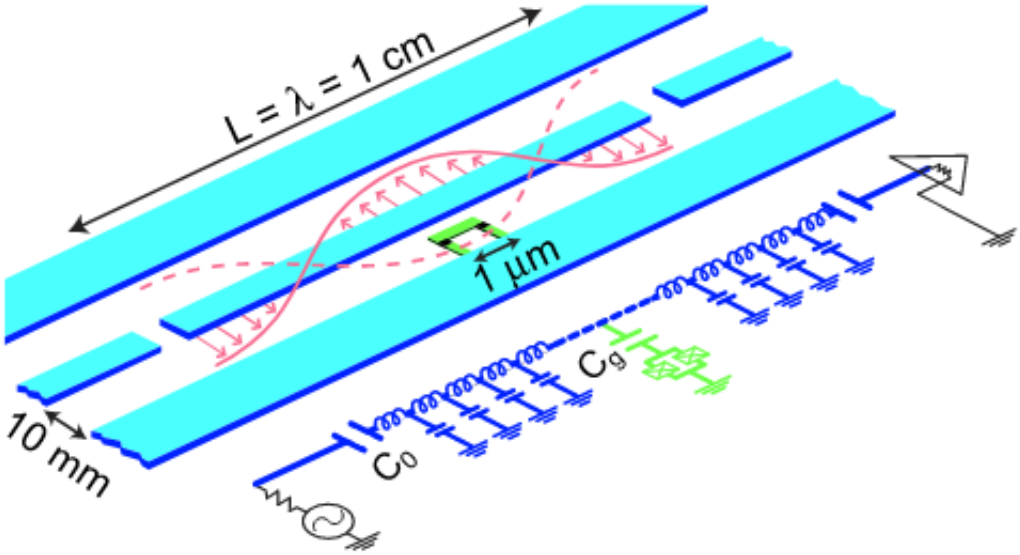

Fig. 2.7 Schematic illustration of a typical coplanar waveguide (CPW) resonator used in circuit QED together with its discretized lumped-element equivalent circuit. The qubit lies between the center pin and the adjacent ground plane and is located at an antinode of the electric field, shown in this case for the full-wave resonance of the CPW. From (Blais *et al.*, 2004).

FIGURE 8: Adapted from: [4]

[h] The discretized circuit is also show on figure 8. For the innitial analysis the qubit and the capacitors C_0 will be ignored. Thus we can assume the current but not the voltage will vanish at the end of the transmission line.

It is convenient to define a new flux variable analogous to the above used but dependent on position.

$$\Phi(x,t) = \int_{-\infty}^{t} d\tau V(x,\tau) \tag{0.0.123}$$

Where $V(x,t) = \partial_t \Phi(x,t)$ is the local voltage on the transmission line at position x and time t. The inductance and capacitance per unit length are l and c respectively. Thus the inductance on a segment is ldx, the voltage drop is $-dx\partial_x\partial_t\Phi(x,t)$ and the flux is $-dx\partial_x\Phi(x,t)$ and the current is $I(x,t) = -\frac{1}{l}\partial_x\Phi(x,t)$. A Lagrangian for a system of length L (not induction) is thus:

$$\mathcal{L}_g = \int_0^L dx\mathcal{L}(x,t) = \int_0^L dx\left[\frac{c}{2}(\partial_t\Phi)^2 - \frac{1}{2l}(\partial_x\Phi)^2\right] \tag{0.0.124}$$

The Euler-Lagrange equation for this Lagrangian is simply the wave equation:

$$v_p^2\partial_x^2\Phi - \partial_t^2\Phi = 0 \tag{0.0.125}$$

The momentum conjugate to $\Phi(x)$ is simply the charge density

$$q(x,t) = \frac{\delta\mathcal{L}_g}{\delta\partial_t\Phi} = c\partial_t\Phi = cV(x,t) \tag{0.0.126}$$

And finally the Hamiltonian:

$$H = \int_0^L dx\left\{\frac{1}{2c}q^2 + \frac{1}{2l}(\partial_x\Phi)^2\right\} \tag{0.0.127}$$

Considering the classical normal mode solutions of the wave equation 0.0.125 we get:

$$\Phi(x,t) = e^{-i\omega t}\phi(x) \tag{0.0.128}$$

We arrive at the Schrodinger like eigenvalue problem:

$$-\partial_x^2\phi(x) = k^2\phi(x) \tag{0.0.129}$$

Where $k = \omega/v_p$ and the mode wave velocity is $v_p = \frac{1}{\sqrt{le}}$. The open-circuit model with zero current at the bondaries tells us that eigenfunctions have vanishing derivative at the boundaries. The normalization chosen is to keep the equation looking as close to those of a single harmonic oscillator.

$$\phi_n(x) = \sqrt{2}\cos(k_n x) \tag{0.0.130}$$

where $n \in \{0,1,2,3,...\}$ and $k_n = \frac{n\pi}{L}$. Because the operator ∂_x is self-adjoint for these boundary conditions and because the eigenvalues are non-degenerate the eigenfuction have the following helpful properties:

$$\int_0^L dx\phi_n(x)\phi_m(x) = L\delta_{nm} \tag{0.0.131}$$

$$\int_0^L dx[\partial_x\phi_n(x)][\partial_x\phi_m(x)] = Lk_n^2\delta_{nm} \tag{0.0.132}$$

From this it follows that the Lagrangian can be diagonalized using these spatial normal modes as basis(because they zero at non diagonal-equal indexes). The field parametrized becomes:

$$\Phi(x,t) = \sum_{n=0}^{\infty} {}_n(t)\phi_n(x) \tag{0.0.133}$$

Where ${}_n$ are arbitrary functions of time (not necessarily complex exponentials).

Then we substitute this equation in the Lagrangian 0.0.124 and using the properties

$$\mathcal{L}_g = \frac{1}{2}Lc\sum_{n=0}^{\infty}[\partial_t {}_n]^2 - \omega_{nn}^{2\,2}{}_{}^{} \tag{0.0.134}$$

We can see that each normal mode in the sum is an independent harmonic oscillator. The momentum conjugate to the normal mode amplitude is:

$$q_n = \frac{\delta\mathcal{L}_g}{\delta\partial_t {}_n} = Lc\partial_t {}_n \tag{0.0.135}$$

And the Hamiltonian is then:

$$\hat{H} = \frac{1}{2}\sum_{n=0}^{\infty}\left\{\frac{1}{Lc}\omega_{nn}^{2\,2}{}_{}^{}\right\} \tag{0.0.136}$$

We can quantize this. The n=0 mode is just a free particle because the 'spring constant' is zero. In that case the momentum(charge) is constant and the position(flux) increases linearly with time. In most cases it can be ignored because the total charge is a constant and typically vanishes.

We end up with a set of independant normal modes with coordinate ${}_n$ and conjugate momentum q_n which when quantized can be expressed in terms of mode raising and lowering operators:

$$\hat{}_n = \sqrt{\frac{\hbar}{2\omega_n Lc}}(\hat{a}_n + \hat{a}_n^\dagger) \tag{0.0.137}$$

$$\hat{q}_n = -i\sqrt{\frac{\hbar\omega_n Lc}{2}}(\hat{a}_n - \hat{a}_n^\dagger) \tag{0.0.138}$$

Where these ladder opperators obey:

$$[\hat{a}_n, \hat{a}_n^\dagger] = \delta_{nm} \tag{0.0.139}$$

If we couple a qubit to a ressonator at x, we need to express the flux and charge density operators at that point in terms of the normal operators:

$$\hat{\Phi}(x) = \sum_{n}^{\infty}\phi_n(x)\hat{}_n \tag{0.0.140}$$

$$\hat{q}(x) = \frac{1}{L}\sum_{n}^{\infty}\phi_n(x)\hat{q}_n \tag{0.0.141}$$

The voltage operator is just:

$$\hat{V}(x) = \frac{1}{c}\hat{q}(x) \tag{0.0.142}$$

The commutation relation is:

$$[\hat{q}(x), \hat{\Phi}(x')] = -i\hbar \frac{1}{L} \sum_{n}^{\infty} \phi_n(x)\phi(x') = -i\hbar\delta(x' - x) \tag{0.0.143}$$

The Hamiltonian now becomes:

$$\hat{H} = \int_0^L dx \left\{ \frac{1}{2c}\hat{q}^2 + \frac{1}{2l}(\partial_x \hat{\Phi})^2 \right\} \tag{0.0.144}$$

Like the classical example of plucking a string we can coherently displace a linear combination of the normal modes.

Suppose we want to displace the resonator's degrees of freedom so that the local displacement obeys:

$$\langle \hat{\Phi}(x) \rangle = \Delta(x) \tag{0.0.145}$$

Where Δ is a specified function. The analog of the displacement operator for the coherent states used before is just:

$$U_\Delta = e^{-\frac{i}{\hbar}\int_0^L dx \Delta(x)\hat{q}(x)} \tag{0.0.146}$$

Superconducting Qubits

So far in studying the Cooper pair box a phenomenon has been ignored that is the build up of charge on the islands as current flows through the junction. Creating a Coulomb energy like a capacitor which makes it into a very good artificial atom.

There are many different kinds of superconducting qubits using the Josephson Junction such as the Cooper pair box based on charge, the flux qubit, the phase qubit and the fluxonium qubit. The works covering those are referenced in [4] chapter 4. These can be classified in a periodic table 9 that shows their differences in the rations of energies and inductance of the Josephson junction.

[h]

The Cooper pair box The cooper pair box (CPB) is topologically exceptional comparing to the other junctions given that it has no wire closing in the loop around the junction.The number of Cooper pairs transferred through the junction is a well defined integer. For this case the system is sensitive to stray electric field noise which is overcome by moving it down in the table 9 towards the transmon. Where the tunneling energy (E_J) dominates the coulomb charging energy(E_c). The charging energy for a single electron is defined as:

$$E_C = \frac{e^2}{2C_\Sigma} \tag{0.0.147}$$

Where $C_\Sigma = C_J + C_g$ is the total capacitance between the islands. Illustrated in 10.

[h]

The Coulomb energy to transfer a Cooper pair is four times that of an electron so we get the Coulomb energy operator:

$$\hat{U} = 4E_C(\hat{n} - n_g)^2 \tag{0.0.148}$$

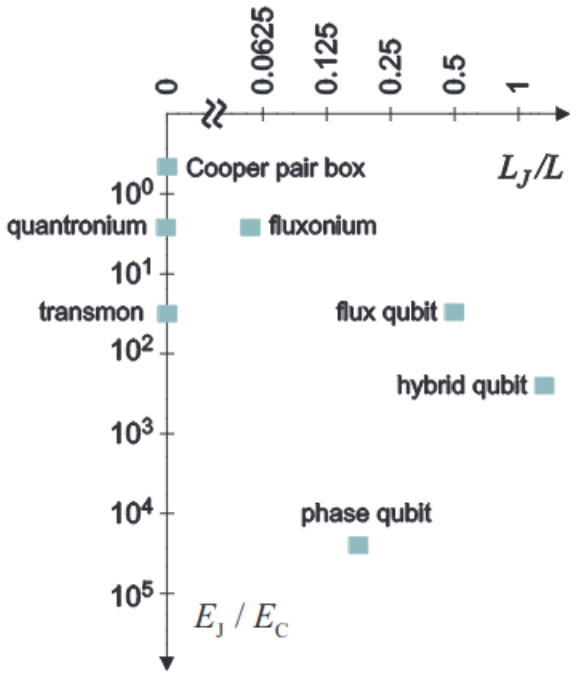

Fig. 4.4 'Periodic Table' of superconducting qubits. E_J is the tunneling Josephson energy, $4E_C$ is the energy cost to charge the junction with one Cooper pair, and $E_L/2$ is the energy cost to 'charge' the shunt inductor with one flux quantum. (Courtesy M. Devoret.)

FIGURE 9: Adapted from: [4]

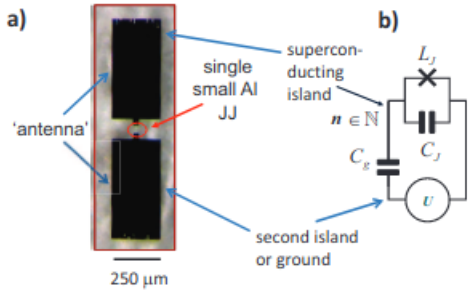

Fig. 4.1 a) Cooper pair box qubit (R. Schoelkopf lab) and b) its equivalent circuit showing a voltage source biasing the box through a coupling ('gate') capacitor c_g. The cross denotes the Josephson junction. The voltage source may represent an intentionally applied bias or be the result of random charges in the insulating substrate supporting the device. The particular device illustrated in (a) is a transmon qubit in a 3D cavity for which there is no dc bias applied (although there may be a random offset voltage due to charges trapped in the substrate).

FIGURE 10: Adapted from: [4]

Where $n_g = -\frac{C_g V}{2e}$ is the dimensionless gate charge or offset charge that represents a break of degeneracy between the transfer of positive and negative charges caused by

an external electric field or some junction asymmetry. It also fluctuates randomly (or intentionally). The phase difference of the junction φ is compact. This means $|\varphi + 2\pi\rangle = |\varphi\rangle$. The number operator is the conjugate angular momentum of φ in the representation is given by:

$$\hat{n} = +i\frac{d}{d\varphi} \tag{0.0.149}$$

The Hamiltonian thus becomes:

$$H = 4E_C(\hat{n} - n_g)^2 - E_J \cos\varphi \tag{0.0.150}$$

In an analogy with a pendulum the charging energy(E_C) is the inverse momentum of inertia and the Josephson energy (E_J) is the torque produced by gravity. For small amplitudes the classical pendulum is basically an harmonic oscillator. We can get a new approximated hamiltonian by expanding the cosine to second order:

$$H \approx 4E_C n^2 + \frac{1}{2}E_J\varphi^2 \tag{0.0.151}$$

From 0.0.41 and the $V(t) = \int_1^2 E(\mathbf{r}, t)d\mathbf{l} = \frac{\partial\Phi(t)}{\partial t}$ relation

$$\frac{\partial\varphi}{\partial t} = \frac{2\pi}{\Phi_0}\int_1^2 \mathbf{E}(\mathbf{r}, t)\cdot d\mathbf{l} = \frac{2\pi}{\Phi_0}V_{1-2}(t) = \frac{2\pi}{\Phi_0}\frac{\partial\Phi}{\partial t} \tag{0.0.152}$$

Thus the phase angle is directly proportional to the flux in the junction:

$$\varphi = \frac{2\pi}{\Phi_0}\Phi \tag{0.0.153}$$

This means that each time the flux variable changes by one flux quantum (Φ_0) the phase difference changes by 2π. And the Hamiltonian becomes:

$$H = \frac{1}{2C}Q^2 - E_J\cos\left(2\pi\frac{\Phi}{\Phi_0}\right) \tag{0.0.154}$$

That approximated is:

$$H = \frac{1}{2C}Q^2 + \cos 2\pi\frac{1}{2L_J}\Phi^2 \tag{0.0.155}$$

Where $L_J = \left(\frac{\hbar}{2e}\right)^2\frac{1}{E_J}$. And approximated this way the CPB becomes a simple harmonic oscillator with resonant frequency(Josephson plasma frequency) given by

$$\omega_J = \frac{1}{\sqrt{L_J C}} = \frac{1}{\hbar}\sqrt{8E_J E_C} \tag{0.0.156}$$

For a general flux Φ we can define a differential inductance:

$$L^{-1}(\Phi) = \frac{d^2H}{d\Phi^2} = E_J\left(\frac{2\pi}{\Phi_0}\right)\cos\left(2\pi\frac{\Phi}{\Phi_0}\right) \tag{0.0.157}$$

Here we see that the Josephson junction acts as a non-linear inductor. This will make the energy levels of the CPB anharmonic like an atom. The reason we call such a device an artificial atom.

We can use this picture of a nonlinear inductor if the zero point fluctuations are small. But in general it's necessary to resort to numerical diagonalization of the CPB Hamiltonian.

For the full Hamiltonian in the hase basis the Schrödinger eigenvalue equation is the Matthieu equation whose solutions are composed in terms of Matthieu functions. The numerical diagonalization is more conveniently performed in the charge(number) basis where the Coulomb term is the diagonal and the Josephson term is tridiagonal ($\langle m \pm 1|\cos\varphi|m\rangle = 1/2$. m are the eigenvalues of the operator $\hat{n}$ and are the labels of the eigenstates. The Hilbert state is truncated at some level $|m| = m_{max}$ that can be estimated from the zero point fluctuations of the charge:

$$m_{max} \gg \sqrt{N}\frac{Q_{ZPF}}{2e} \approx \sqrt{N}\left(\frac{E_J}{32E_C}\right)^{1/8} \tag{0.0.158}$$

The qubit spectrum is periodic in the offset charge n_g. So this means we can cancel the integer part of it by exchanging a integer number of Cooper pairs.

The unitary transformation:

$$U_\pm = e^{\varphi} \tag{0.0.159}$$

Preserves the boundary conditions but shifts the angular momentum (transferred charge) by one unit

$$U_\pm \hat{n} U_\pm^\dagger = \hat{n} \mp 1 \tag{0.0.160}$$

The pendulum analogy doesn't hold for the offset n_g. But we can consider it goes under an Aharanov-Bohm phase shift as it circles a line of (fake) magnetic flux. The same way we substitute the canonical momentum for the mechanical momentum of a charged particle.

$$\mathbf{p} \rightarrow \mathbf{p} - q\mathbf{A}(\mathbf{r}) \tag{0.0.161}$$

For our pendulum turning on the z axis we use the angular momentum:

$$L_z = (\mathbf{r}\times\mathbf{p}) \rightarrow (\mathbf{r}\times\mathbf{p})_z - q(\mathbf{r}\times\mathbf{A})_z \tag{0.0.162}$$

Considering a magnetic field that is null everywhere but this Aharanov-Bohm tube on the z axis the gauge we can chose is:

$$\mathbf{A}(\mathbf{r}) = \Phi_{AB}\frac{1}{2\pi r}\hat{z}\times\hat{r} \tag{0.0.163}$$

Which has the correct total flux:

$$\oint \mathbf{A}\cdot d\mathbf{r} = \Phi_{AB} \tag{0.0.164}$$

For any loop with +1 winding number around z. The mechanical angular momentum is thus:

$$(\mathbf{r}\times\mathbf{p})_z - \frac{q}{2\pi}\Phi_{AB} = \hbar\left(-i\frac{\partial}{\partial\varphi} - \frac{\Phi_{AB}}{\Phi_0}\right) \tag{0.0.165}$$

Comparing it with the Hamiltonian 0.0.150 we see that the offset charge is equivalent fo the fake Aharonov-Bohm flux $n_g = \frac{\Phi}{\Phi_0}$

In the charge limit $E_C \gg E_J$ the states are nearly angular momentum states weakly perturbed by the Josephson coupling (gravitational force in the analogy). You can see how at this charge limit end the states in blue and red overlap when the charge is half-integer (figure **??**). Also since the factor E_C is big the excitation energies are influenced by a large extent by n_g which is a noisy factor.

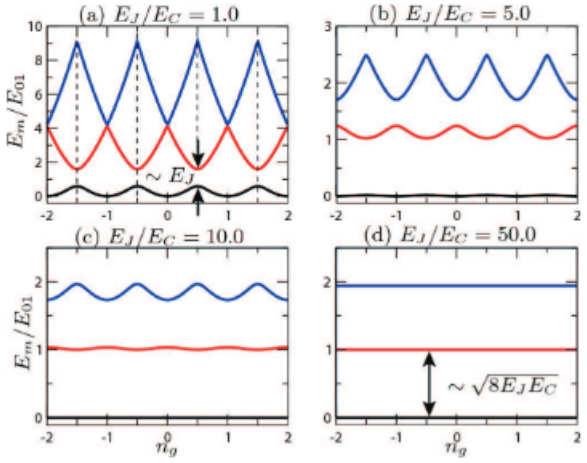

Fig. 4.6 Energy spectrum of the Cooper pair box as a function of offset charge for different values of the dimensionless ratio of Josephson energy to charging energy. The exponential decrease in the charge dispersion is clearly seen. From (Koch *et al.*, 2007).

FIGURE 11: Adapted from: [4]

[h]

On the other hand for the E_{JC} limit, the transmon limit. The pendulum motion are small amplitude harmonic oscillator like. Because now the gravitational force (out of the analogy E_J) is much more significant. The susceptibility to noise is much smaller too. Because for the fake Aharanov-Bohm flux to influence the pendulum, it has to complete an entire lap. And now the barrier that the system has to tunnel from 0 to 2π is much greater and it's height proportional to E_J. And the particle 'mass' is also proportional to $1/E_C$.

Back to the language of wave function. We start with this unitary transformation that removes the offset charge term from the hamiltonian:

$$U = e^{-in_g\varphi} \tag{0.0.166}$$

$$U(\hat{n} - n_g)U^\dagger = \hat{n} \tag{0.0.167}$$

An important detail is that the function does not obey periodic boundary conditions:

$$U\Psi(\varphi + 2\pi) = e^{-i2\pi n_g}U\Psi(\varphi) \tag{0.0.168}$$

But the Hamiltonian becomes independent of n_g:

$$UHU^\dagger = H = 4E_C\hat{n}^2 - E_J\cos\varphi \tag{0.0.169}$$

For a large E_J/E_C the wave function is exponentially small at $\varphi = \pm\pi$. So we do not expect a large change in the spectrum due to the change in the boundary condition.

You can see how n_g is less relevant to a junction under these conditions in 11 (d). Where a large E_J/E_C factor has a flat constant energy level to a varying n_g. Although higher energy states can tunnel more easily through the barrier and so will have a higher charge dispersion.

In this limit of large E_J/E_C that the pendulum approaches an harmonic oscillator the anharmonicity defined by:

$$A = \omega_{12} - \omega 01 \approx E_C \tag{0.0.170}$$

goes to zero very slowly as the charging energy is reduced and can be kept above 100-200MHz which is adequate to prevent smooth nanosecond control pulses from taking the qubit to states out of the logical subspace (the two lower levels).

The anharmonicity can be estimated through perturbation theory by expanding the cosine above the second order:

$$H \approx H_0 + V = 4E_C\hat{n}^2 + \frac{1}{2}E_J\hat{\varphi}^2 + (-\frac{1}{24}E_J\hat{\varphi}^4 \tag{0.0.171}$$

Also using $\hat{\varphi} = \varphi_{ZPF}(\hat{a} + \hat{a}^\dagger$ and $\varphi^2_{ZPF} = \sqrt{\frac{2E_C}{E_J}}$ the perturbation term is:

$$V = -\frac{1}{24}E_J\hat{\varphi}^4 = -\frac{1}{12}E_C(\hat{a} + \hat{a}^\dagger)^4 \approx -\frac{E_C}{2}(\hat{a}^\dagger\hat{a}^\dagger\hat{a}\hat{a} + 2\hat{a}^\dagger\hat{a}) \tag{0.0.172}$$

The second term in the final approximation renormalizes the harmonic oscillator frequency slightly down and the first will introduce this anharmonicity $-E_C$:

$$A = \omega_{12} - \omega_{01} = \frac{E_C}{2}\langle 2|(\hat{a}^\dagger\hat{a}^\dagger\hat{a}\hat{a})|2\rangle = \frac{E_C}{2}\sqrt{2}\cdot 1\cdot 1\cdot\sqrt{2} = -E_C \tag{0.0.173}$$

Inductively Shunted Qubits

In the phase qubit the the Josephson junction is shunted by a lumped element inductor. For the fluxonium a large inductance is needed. A value that is impossible to obtain with a coiled wire due to parasitic capacitances and the low value of the fine structure constant. Instead we use a long chain of Josephson junctions. The flux qubit uses only two making the shunting not linear.

The great differences from a inductive shunted qubit to a regular CPB are the φ and $\varphi + 2\pi$ are no longer equivalent because they differ in how much current flows through them. The charge variable now is also not continuous anymore because φ is no longer a compact variable and the system doesn't obey periodic boundary values. So the energy store in the inductor diverges for large $|\varphi|$. Because of these new properties the φ variable will be represented with a hat. The new hamiltonian is:

$$H = 4E_C(\hat{n} - n_g)^2 - E_J\cos\hat{\varphi} + \frac{1}{2}E_L\hat{\varphi}^2 \tag{0.0.174}$$

Now with a continuous charge we can eliminate n_g completely. And the spectrum will not depend on the static offset of the charge in any way for the transformed wave function $U\Psi$. Since:

$$E_L = \left(\frac{\hbar}{2e}\right)^2 \frac{1}{L} = \left(\frac{\Phi_0}{2\pi}\right)^2 \frac{1}{L} \tag{0.0.175}$$

If we take the limit $L \to \infty$ that implies $E_L \to 0$ the phase variable will no longer be compact but the term with the E_L will no longer affect the Hamiltonian. Physically the high frequency oscillations of the qubit aren't affected but there is a continuous k of states instead of discreet ones.

n_g doesn't affect the spectrum anymore because it only shifts the states $k \to k + n_g$ but all values of k are allowed and the function is periodic $k \to k + 1$.

If the inductive energy is non zero the Bloch theorem doesn't apply anymore. The interplay between the quadratic term and the cosine from the Josephson term allows us to create many different potential wells shapes and generate an interesting spectra of qubits.

We can also control the externally applied flux which would be the inductive analog of the offset charge n_g and will be called φ_g. The Hamiltonian is now:

$$H = 4E_C(\hat{n} - n_g)^2 - E_J \cos\hat{\varphi} + \frac{1}{2}E_L(\hat{\varphi} - \varphi_g)^2 \tag{0.0.176}$$

We can translate these offsets using an unitary transformation:

$$U = e^{i\varphi_g \hat{n}} e^{i\hat{\varphi} n_g} \tag{0.0.177}$$

The hamiltonian then becomes:

$$H = 4E_C(\hat{n})^2 - E_J \cos(\hat{\varphi} + \varphi_g) + \frac{1}{2}E_L(\hat{\varphi})^2 \tag{0.0.178}$$

We see now that the spectrum must be periodic in the offset flux.

To summarize the control knobs the experimentalist has are the variables: E_J, E_C, E_L and n_g. Which allow us to create a rich variety of level structures.

The phase qubit operates around $E_J/E_C \approx 10^4$ which makes it very nearly an harmonic oscillator. To make it aharmonic a large flux bias is used on the inductor. But this also makes the energy level spacing small. So the junctions have a large area and a Josephson plasma frequency of $\omega_L = \sqrt{8E_J E_C}/h$ which is very high and around 50GHz.

[h]

In the Fluxonium qubit the large inductance is supplied by an array of Josephson junctions that generate a kinetic inductance. The anharmonicity can also be large.

In figure 12 (c) we can see the configuration of the potential well of the fluxonium for $\varphi_g = 0$. The ground state is supported by the middle valley and there are two excited states to the left and right. This is known as V configuration. For 12 (a) there are two low states with a large gap to the next excited state. This is known as a '$Lambda$' configuration. For 12 (b) finally the fluxonium varies smoothly between these two limits and does not have exponential sensitivity to external flux unlike the flux qubit.

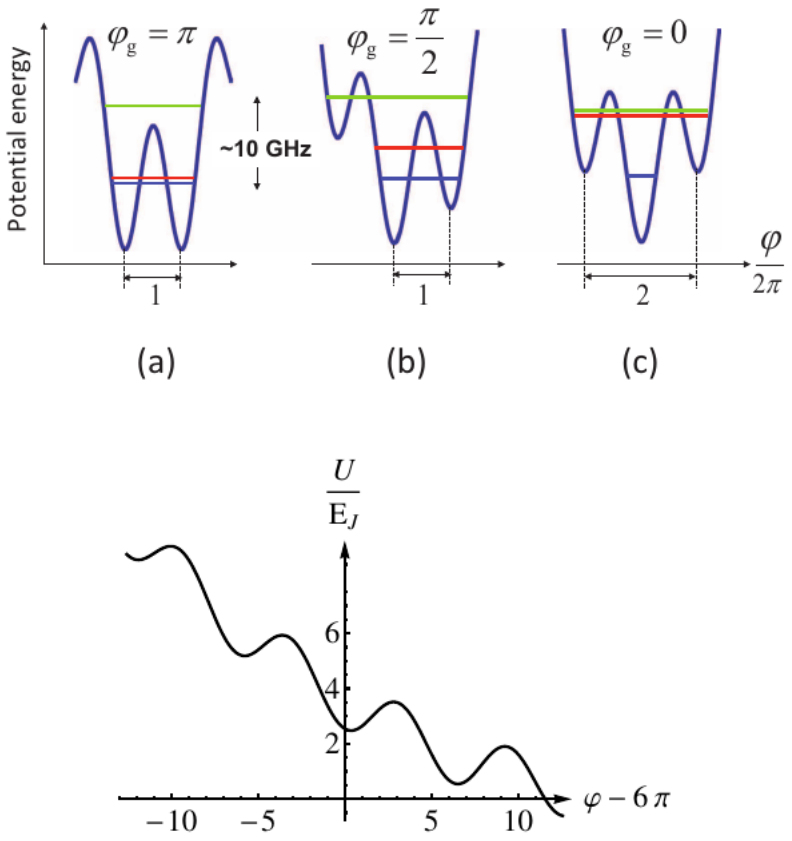

Fig. 4.8 a) Extended cosine potential $U = -E_J \cos(\varphi + \varphi_g) + E_L\varphi^2$, with dimensionless offset flux $\varphi_g = \pi$. Used in the fluxonium qubit to produce a 'Λ' level configuration; b) Same as (a) but with $\varphi_g = \pi/2$; c) Same as (a) but with $\varphi_g = 0$ to produce a 'V' level configuration; (bottom panel) Same as (a) but displaced a distance $\varphi_g = 6\pi$ to illustrate the current (flux) biased phase qubit. $E_L = 0.01E_J$.

FIGURE 12: Adapted from: [4]

Introduction to Cavity and Circuit QED

Cavity QED is about controlling the quantum fluctuations of the vacuum by creating a resonant cavity that supports discrete modes of an electromagnetic field. One can alter the coupling of the atoms to their quantum environment by altering the frequencies and damping of the cavity. Because of the interaction of the photons in the cavity to the atoms one can enter a coherent superposition of these photons and the atom called *polaritons*. Using optical frequencies it's not possible to measure the state of the atom because the lifetime of spontaneous emission is of the order of nanoseconds. Though using microwaves the lifetime can be increased to around 30ms.

[h]

Circuit QED uses superconducting qubits as artificial atoms coupled to microwave resonators (figure 13). Measuring the amplitude and the phase of microwaves transmitted (reflected) through the resonator.

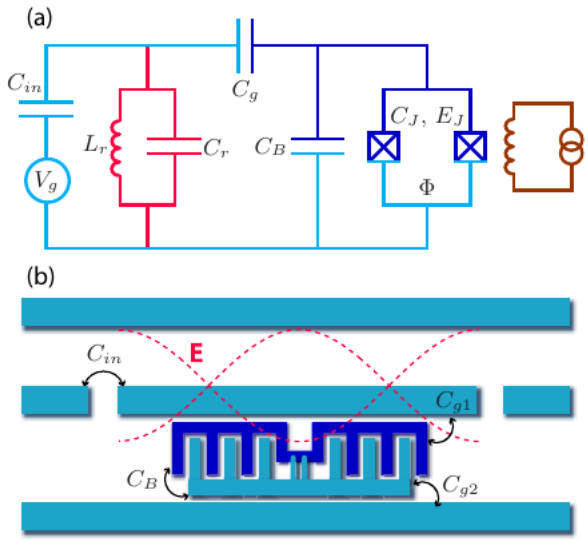

Fig. 6.1 Circuit QED: Schematic illustration (not to scale) of a transmon qubit embedded in a coplanar waveguide resonator. Panel (a) shows the lumped element circuit equivalent to the distributed circuit shown in panel (b). From (Koch *et al.*, 2007).

FIGURE 13: Adapted from: [4]

Application of microwaves near the cavity frequency excites de cavity and performs a measurement while a microwave at the qubit transition frequency does not excite the cavity nor causes a measurement. These waves can be used to perform single qubit rotations.

In optical cQED a Frabry-Pérot cavity is used which is typically very large compared to optical wavelengths associated with atomic spectra.

In circuit QED coupling can be arbitrarily strong because the antennae can be made as big as desired. The challenge is to obtain weak coupling to protect the qubit from the environmental noise by filtering it. The phyiscs of using a cabity to modify the coupling is that of a Purcell effect where a qubit is placed inside a cavity can have it's decay rate controlled by how far detuned or close from the cavity resonance. Which is useful for protecting superpositions in low detuning or for reseting the qubit with high detuning. It can also be used to create single microwave photons on demand and enhance the transfer of quantum information from the artificial atom to the cavity photon. One can view the Purcell effect as the resonator performs an impedance transformation on the external dissipation of the environment to the qubit.

The coupling between the electric field in the cavity and the dipole moment of a single atom at $\mathbf{r}$ is:

$$U = -\mathbf{p} \cdot \mathbf{E}(\mathbf{r}) \tag{0.0.179}$$

We assume that only the cavity HO mode close to the atom transition frequency is important. The electric field at $\mathbf{r}$ can be written in terms of the mode polarization directing $\hat{\epsilon}$ and the zero point fluctuation E_{ZPF} at $\mathbf{r}$

$$\mathbf{E} = \hat{\epsilon} E_{\text{ZPF}} (\hat{a} + \hat{a}^{\dagger}) \tag{0.0.180}$$

Since the dipole moment operator connects to the ground and excited states of the two level atom the interaction Hamiltonian becomes:

$$H_1 = \hbar g(\hat{a} + \hat{a}^\dagger)\sigma_x \tag{0.0.181}$$

Where σ_x toggles the atom's states and g is the vacuum Rabi coupling given by the dipole matrix:

$$\hbar g = \langle \Psi_1 | \mathbf{p} \cdot \hat{\epsilon} | \Psi_0 \rangle E_{\text{ZPF}} \tag{0.0.182}$$

The interaction Hamiltonian can be rewritten as:

$$H_1 = \hbar g(\hat{a}\sigma_+ + \hat{a}^\dagger\sigma_-) + \hbar g(\hat{a}\sigma_- + \hat{a}^\dagger\sigma_+) \tag{0.0.183}$$

Where:

$$\sigma_\pm = \frac{1}{2}(\sigma_x \pm i\sigma_y) \tag{0.0.184}$$

We drop the second term of the equation 0.0.183 which is called doing a rotating wave approximation (RWA) because which is valid if the coupling is not very strong or if the detuning is so large that no cavity mode is singled out. We can do this because the second term doesn't conserve the energy, a photon is created(destroyed) and the cavity also goes to the excited (ground) state and so is much less likely under those conditions. The simplest approximation is using the Jaynes Cummings Hamiltonian with

$$H_0 = \hbar\omega_C \hat{a}^\dagger \hat{a} + \frac{\hbar\omega_{01}}{2}\omega_z \tag{0.0.185}$$

$$V = \hbar g(\hat{a}\sigma_+ + \hat{a}^\dagger\sigma_-) \tag{0.0.186}$$

The full hamiltonian is thus:

$$H_0 = \hbar\omega_C \hat{a}^\dagger \hat{a} + \frac{\hbar\omega_{01}}{2}\omega_z + \hbar g(\hat{a}\sigma_+ + \hat{a}^\dagger\sigma_-) + H_{\text{drive}} + H_{\text{dampings}} \tag{0.0.187}$$

Where the two hamiltonians in the end account for the external driving and damping which help control the states of the cavity. Let the detuning between the qubit frequency and the cavity frequency be:

$$\Delta = \omega_{01} - \omega_c \tag{0.0.188}$$

[h]

Starting with $\Delta = 0$ we see in figure 14 (a) that there is a degeneracy of states such as $|1, g\rangle$ and $|0, e\rangle$. But there is also a break of this degeneracy lifted by the dipole coupling matrix element resulting in a $2g\sqrt{n+1}$ split. The split of $2g$ for the lowest pair is called vacuum Rabi splitting.

The energy eigenstates of the Hamiltonian $H_0 + V$ are given by:

$$|\Psi_\pm\rangle = \frac{1}{\sqrt{2}}(|n+1, g\rangle \pm |n, e\rangle) \tag{0.0.189}$$

And called bonding-anti-bonding combinations.

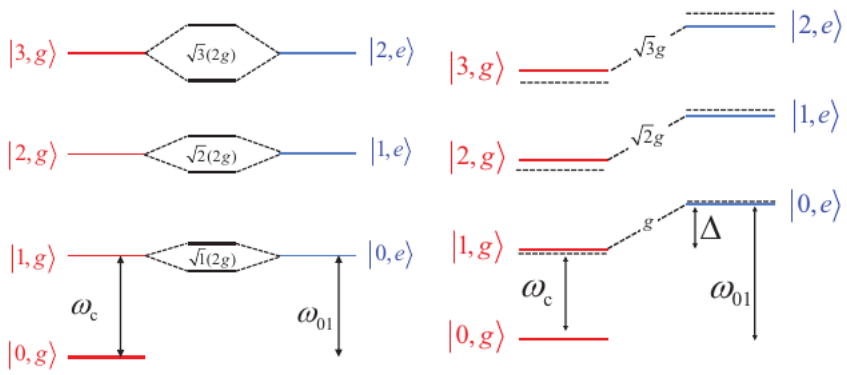

Fig. 6.2 Jaynes-Cummings ladder or 'dressed-atom' level structure. (left panel) Degenerate case $\omega_{01} = \omega_c$. The degenerate levels mix and split by an amount proportional to the vacuum Rabi splitting g. (right panel) Dispersive case $\omega_{01} = \omega_c + \Delta$. For $\Delta > 0$ the level repulsion causes the cavity frequency to decrease when the qubit is in the ground state and increase when the qubit is in the excited state.

FIGURE 14: Adapted from: [4]

In the dispersive regime where $|\Delta| \gg g$ where the qubit is far detuned from the cavity. We will see that the diagonalization of the Hamiltonian to lowest order in g leads to a second-order dispersive coupling.

$$V_{\text{dispersive}} = \hbar \frac{g^2}{\Delta} \left[\hat{a}^\dagger \hat{a} + \frac{1}{2} \right] \sigma_z \tag{0.0.190}$$

This coupling is quantum non-demolition (QND) with respect to photon number and qubit polarization since it commutes with both. The dispersive coupling can be thought as either a shift in the cavity frequency which depends on the state of the qubit or as the ac-Stark light shift of the qubit frequency proportional to the number of photons in the cavity.

The qubit-state-dependant shift of the cavity frequency leads to both changes in amplitude and phase of the reflected from or transmitted through the cavity and is the basis of the qubit readout in QND of the qubit state.

As required by a quantum measurement the photon shot noise in the cavity gradually dephases the qubit superposition as information is gained about σ_z. This is observed as a broadening spectroscopic line width of the qubit.

To derive the Hamiltonian in a dispersive regime (equation 0.0.190) we need to find a unitary transformation which removes the off diagonal term in equation 0.0.186:

$$U = e^{\hat{\eta}} \tag{0.0.191}$$

which is first order in g.

Using the Baker-Campbell-Hausdorff (BCH) expansion we have:

$$\hat{H} = UHU^\dagger = H + [\hat{\eta}, H] + \frac{1}{2}[\hat{\eta}, [\hat{\eta}, H]] + \ldots \tag{0.0.192}$$

Substituting $H = H_0 + V$ from perturbation theory and expanding the BCH only to the second term:

$$\tilde{H} = H_0 + V + [\hat{\eta}, H_0] + [\hat{\eta}, V] + \frac{1}{2}[\hat{\eta}, [\hat{\eta}, H_0]] \tag{0.0.193}$$

$\hat{\eta}$ Is chosen to satisfy:

$$[\hat{\eta}, H_0] = -V \tag{0.0.194}$$

We get then:

$$\tilde{H} = H_0 + \frac{1}{2}[\hat{\eta}, V] \tag{0.0.195}$$

It's easy to verify that eq. 0.0.194 solution is

$$\hat{\eta} = \frac{g}{\Delta}(\hat{a}\sigma_+ - \hat{a}^\dagger\sigma_-) \tag{0.0.196}$$

This expansion is only valid for large enough detuning $g/\Delta \ll 1$. Otherwise the RWA expansion fails. The dispersive Hamiltonian is then:

$$\tilde{H} = H_0 + \hbar\frac{g^2}{\Delta}\left(\hat{a}^\dagger\hat{a} + \frac{1}{2}\right)\sigma_z \tag{0.0.197}$$

Without drive or damping the Hamiltonian will commute with the excitation number that is the sum of the cavity excitation number and the qubit excitation number:

$$\hat{N}_{\text{ex}} = \hat{a}\hat{a}^\dagger + \frac{1+\sigma_z}{2} \tag{0.0.198}$$

The solution then is of the form:

$$\Psi^{(n+1)} = \alpha|n, e\rangle + \beta|n+1, g\rangle \tag{0.0.199}$$

For which the 2×2 eigenvalue problem becomes:

$$H_{2\times2}^{(n+1)}\begin{pmatrix}\alpha\\ \beta\end{pmatrix} = E_\pm^{(n)}\begin{pmatrix}\alpha\\ \beta\end{pmatrix} \tag{0.0.200}$$

Where:

$$H_{2\times2}^{(n+1)} = \left(n + \frac{1}{2}\right)\hbar\omega_c + \hbar\begin{pmatrix}\frac{\Delta}{2} & g\sqrt{n+1}\\ g\sqrt{n+1} & \frac{-\Delta}{2}\end{pmatrix} \tag{0.0.201}$$

The eigenvalues of these equation are:

$$E_\pm^{(n)} = \left(n + \frac{1}{2}\right)\hbar\omega_c \pm \frac{\hbar}{2}\sqrt{\Delta^2 + 4g^2(n+1)} \tag{0.0.202}$$

The eigenfunctions are:

$$\Psi_+ = \begin{pmatrix}\alpha_+\\ \beta_+\end{pmatrix} = \begin{pmatrix}\cos(\theta/2)\\ \sin(\theta/2)\end{pmatrix}$$

(0.0.203)

$$\Psi_- = \begin{pmatrix} \alpha_- \\ \beta_- \end{pmatrix} = \begin{pmatrix} -\sin(\theta/2) \\ \cos(\theta/2) \end{pmatrix}$$

(0.0.204)

Where:

$$\theta = \tan^{-1}\left(\frac{2g\sqrt{n+1}}{\Delta}\right) \tag{0.0.205}$$

Dispersive limit ($g \ll \Delta$) We can do a Taylor expansion of th energy eigenvalues to obtain:

$$E_\pm^{(n)} = \left(n + \frac{1}{2}\right)\hbar\omega_c \pm \hbar\Delta\left[\frac{1}{2} + \left(\frac{g}{\Delta}\right)^2 (n+1) - \left(\frac{g}{\Delta}\right)^4 (n+1)^2\right] \tag{0.0.206}$$

We can reexpress it as an effective Hamiltonian:

$$\tilde{H} = \left(\hat{N}_{ex} - \frac{1}{2}\right)\hbar\omega_c + \Sigma_z\hbar\Delta\left[\frac{1}{2} + \left(\frac{g}{\Delta}\right)^2 (\hat{N}_{ex}) - \left(\frac{g}{\Delta}\right)^4 (\hat{N}_{ex})^2\right] \tag{0.0.207}$$

Where $\Sigma_z = \pm 1$ is a spin label that smoothly connects to σ_z in the limit $g \to 0$.

We can observe that the lowest term is like the dispersive Hamiltonian and the next order term is some aharmonicity inherited from the qubit to the cavity (self-Kerr effect).

$\Delta = 0$ Here the uncoupled levels occur in degenerate pairs that are lifted by an amount proportional to g.

$$E_\pm^{(n)} = \left(n + \frac{1}{2}\right)\hbar\omega_c \pm \hbar g\sqrt{n+1} \tag{0.0.208}$$

The single excitation eigenstates are the polaritons mentioned before. Coherent superpositions of qubit and cavity excitations. The vacuum Rabi splitting can be observed spectroscopically. Because of the peculiar $\sqrt{n+1}$ and the excitation being half qubit half photon the polariton state is quite anharmonic which means we can treat one of the polariton states and the ground state as a two level system in the strong coupling limit. That also can be driven strongly without going up the excitation ladder and can be coherently flopped like a qubit.

Returning to the dispersive limit where the qubit is strongly detuned from the cavity. One polariton has primarily qubit character and the other primarily cavity character.

For the case of positive detuning it is $\Psi_=^{(n=0)}$ which is primarily qubit. The rate of relaxation of this state is giving by the weighted averages of the bare qubit and cavity decay rates:

$$\gamma_{\text{tot}} = \cos^2(\theta/2)\gamma + \sin^2(\theta/2)\kappa \tag{0.0.209}$$

Where κ is the cavity line width and γ is the atom line width. θ is from the equation 0.0.205. For large detuning where $\sin^2(\theta/2)$ is small. The spontaneous emission of a photon via the cavity is very weak. We can say that the qubit must emit it's fluorescence photon into the cavity and pay the energy denominator price of a large detuning. Equivalently the cavity will filter out the vacuum noise at the qubit frequency which otherwise would cause fairly rapid spontaneous emition.

Quantum control of Qubits in Cavities

Suppose we apply a classical drive with a smooth envelope centered on the qubit transition frequency $\omega 01$ to the cavity:

$$V_d = \{v_R(t)\cos\omega_[01]t + v_R(t)\sin\omega_[01]t\}(\hat{a}^\dagger + \hat{a}) \tag{0.0.210}$$

In the dispersive regime this drive is far removed from the cavity resonance and only weakly populates the cavity with virtual photons. The vacuum Rabi coupling term of the Jaynes-cummongs model in equation 0.0.186 can then cause coherent rotations of the qubit. This is most easily analyzed by applying the dispersive unitary transformation of equation 0.0.191. To lowest order in g/Δ we have the original rive on the cavity plus an effective drive directly on the qubit:

$$\tilde{V}_d \approx V_d + Vdq \tag{0.0.211}$$

Where:

$$V_{dq} = [\eta, V_d] = \{_R(t)\cos\omega_{01}t + \lambda_I(t)\sin\omega_{01}t\}\sigma_x \tag{0.0.212}$$

For large detuning ($\Delta \gg \kappa, \chi$) the complex qubit drive amplitude given by

$$\lambda_R(I) = v_{R(I)}(t)\frac{g}{\Delta} \tag{0.0.213}$$

can be interpreted as the external drive filtered by the response function of the cavity. (note that the filter factor is the same independent of the state of the qubit because $\Delta \gg \chi$.

We apply a unitary to take us into the rotating frame at the qubit transition frequency.

$$U_{rot} = e^{\frac{i}{2}\omega_{01}t\,\sigma_z} \tag{0.0.214}$$

And we are left with:

$$H_{rot} = U_{rot}HU_{rot}^\dagger = \frac{\lambda_R(t)}{2}\sigma_x - \frac{\lambda_I(t)}{2}\sigma_y \tag{0.0.215}$$

Thus we see that the cosine and sine drives produce rotations of the qubit around the x and y axes (in the rotation frame). Rotations in the z axis can be obtained in software by a combination of x and y rotations or in hardware by manipulating the qubit frequency to speed up or slow down the precession. This gives us total control over the qubit state.

We have demonstrated that a single input wire to the cavity can be frequency multiplexed. A drive near the cavity frequency produces a dispersive measurement of the qubit state because the resonance frequency of the cavity and hence the reflection coefficient depends on the state of the qubit.

On the other hand a drive at the qubit frequency is so far detuned from the cavity frequency that reflection coefficient is independent of the state of the qubit and so almost no measurement (or measurement induced dephasing) occurs with coherent control pulses to rotate the qubit.

Qutip Jupyter notebook with a CNOT gate made of iSWAPs

This section is a jupyter notebook that can be found on Github (link) that simulates using Qutip a cavity plus two qubits system. That is controlled to do a series of one gate and two gates operations to obtain the equivalent of applying a CNOT gate plus some one qubit gate operations. Described with better details on the notebook:

References quoted in this notebook are Krantz's A quantum engineer's guide to superconducting qubits [7] and Wolfowicz's Pulse Techniques for Quantum Information Processing [9].

```
%matplotlib inline

from qutip import *
from math import *

import matplotlib.pyplot as plt
import numpy as np

from IPython.display import Image
```

Model for two driven directly coupled qubits

In the notebook I will demonstrate a simulation of two qubits using a time dependant hamiltonian. Starting with a series of gates that will go back and forth to $|0\rangle$ to demonstrate the 1 qubit gates.

Ending with another NOT gate on qubit 2, a Hadamard on qubit 1 and, the 2 qubit gate with a simple coupling, a CNOT2,1 (NOT on 2 controlled by 1). To get to finally the cat state: $|\Psi\rangle = \frac{1}{\sqrt{2}}|01\rangle + \frac{1}{\sqrt{2}}|10\rangle$

Based on: https://nbviewer.ipython.org/github/jrjohansson/qutip-lectures/blob/master/Lecture-2A-Cavity-Qubit-Gates.ipynb

Constants

```
w1 = 3.0 * 2 * pi #qubit 1 angular freq
w2 = 2.0 * 2 * pi #qubit 2 angular freq

g = 0.01 * 2 * pi
```

```
Omega1=4
Omega2=4

time_interval=40
points=1600
pntperns=ceil(points/time_interval)

tlist = np.linspace(0, time_interval, points)

width = 0.5

#rotating wave approximation
use_rwa= False
```

Operators

```
sm1 = tensor(destroy(2), qeye(2))

sz1 = tensor(sigmaz(), qeye(2))
sy1 = tensor(sigmay(), qeye(2))
sx1 = tensor(sigmax(), qeye(2))
n1 = sm1.dag() * sm1

# operators for qubit 2
sm2 = tensor(qeye(2), destroy(2))

sz2 = tensor(qeye(2), sigmaz())
sy2 = tensor(qeye(2), sigmay())
sx2 = tensor(qeye(2), sigmax())
n2 = sm2.dag() * sm2
```

Components of the Hamiltonian

```
# Hamiltonian using QuTiP

#qubits
H1 = - 0.5 * sz1 * w1
H2 = - 0.5 * sz2 * w2

#qubit drives
Hd1=Omega1*sy1
Hd2=Omega2*sy2

#Qubit coupling hamiltonian
# Hamiltonian
if use_rwa:
```

```
    Hqq = -g/2 * (sx1*sx2+sy1*xy2)
else:
    Hqq = -g * (sm1.dag() - sm1) * ( sm2.dag()-sm2)

H = H1 + H2 +Hqq + Hd1+Hd2
```

Hamiltonian without rotating wave approximation:

$$H = \frac{\omega_1}{2}\sigma_{z1} + \frac{\omega_2}{2}\sigma_{z2} - g(\sigma_{+1} - \sigma_{-1})(\sigma_{+2} - \sigma_{-2}) + V_{d1}(t)\Omega_1\sigma_{y1} + V_{d2}(t)\Omega_2\sigma_{y2}$$

```
H
```

Quantum object: dims = [[2, 2], [2, 2]], shape = (4, 4), type = oper, isherm = True

$$\begin{pmatrix} -15.708 & -4.0j & -4.0j & -0.063 \\ 4.0j & -3.142 & 0.063 & -4.0j \\ 4.0j & 0.063 & 3.142 & -4.0j \\ -0.063 & 4.0j & 4.0j & 15.708 \end{pmatrix}$$

Dissipation

```
dissipation=True
gamma1 = 0.0033
gamma2 = 0.005

if dissipation:
    c_ops = [sqrt(gamma1) * sm1, sqrt(gamma2) * sm2]
else:
    c_ops=[]

#unitary step function
def u_t(t):
    return 1*(t > 0)
```

We use Krantz's "A quantum engineer's guide to superconducting qubits" page 28 to calculate the lenghts of the pulses. The drive appears in the hamiltonian at the terms for each qubit:

$H_d = V_d(t)\Omega\sigma_y$

The Drive voltage input is a sine wave with amplitude V_0 angular frenquency ω_d, phase ϕ and $s(t)$ is a package envoltory that will be a rectangular function here:

$V_d(t) = V_0 s(t)\sin(\omega_d t + \phi)$

A V_d pulse with ω_d angular frequency resonant to the target qubit frequency makes an unitary transformation like this:

$U = e^{-i/2\Theta(t)(I\sigma_x + Q\sigma_y)}$

Where $I = \cos\phi$ is the in phase factor and $Q = \sin\phi$ is the out of phase factor.

The angle $\Theta(t)$ which is the angle by which the qubit state is rotated is given by:

$\Theta(t) = -\Omega V_0 \int_0^t s(t')dt'$

This equation can be used to tune the inputs like the amplitude V_0 and the integral of the envelope $s(t)$ which will be in our case the period of the rectangular function to obtain a desired angle like π.

By doing the drive voltage completely in phase or out of phase we get the following unitaries:

$U_{I=1,Q=0} = \cos(\frac{\Theta(t)}{2}) + i\sin(\frac{\Theta(t)}{2})\sigma_x = (\Theta)_X$

$U_{I=0,Q=1} = \cos(\frac{\Theta(t)}{2}) + i\sin(\frac{\Theta(t)}{2})\sigma_y = (\Theta)_Y$

The in phase turns the qubit Θ degrees on the x axis and so does the out of phase but on the y axis.

This can then be used to make the X (in phase π degrees) and Y (out of phase π degrees) gates:

$X = \sigma_x = i\sigma_x = U_{I=1,Q=0,\Theta=\pi} = (\pi)_X$

$Y = \sigma_y = i\sigma_y = U_{I=0,Q=1,\Theta=\pi} = (\pi)_Y$

The i is ignored because it's a global phase which can be ignored for not altering the results of measurements.

The Final Pauli gate the Z gate (a rotation on the qubit's Z axis) can be obtained by a combination of three gates where X means in phase (rotation around x axis) and Y out of phase pulses:

$\theta_Z = (\pi/2)_X\theta_Y(-\pi/2)_X = (\pi/2)_X\theta_Y(3\pi/2)_X$

This equation is from: https://www.ucl.ac.uk/quantum-spins/sites/quantum-spins/files/paper90.pdf page 1516 eq2

The bloch sphere below can aid in visualizing the rotations. The rotations follow the right hand rule with the thumb pointed to the positive direction in the axis:

```
Image(filename='images/notebook-bloch-sphere.png')
```

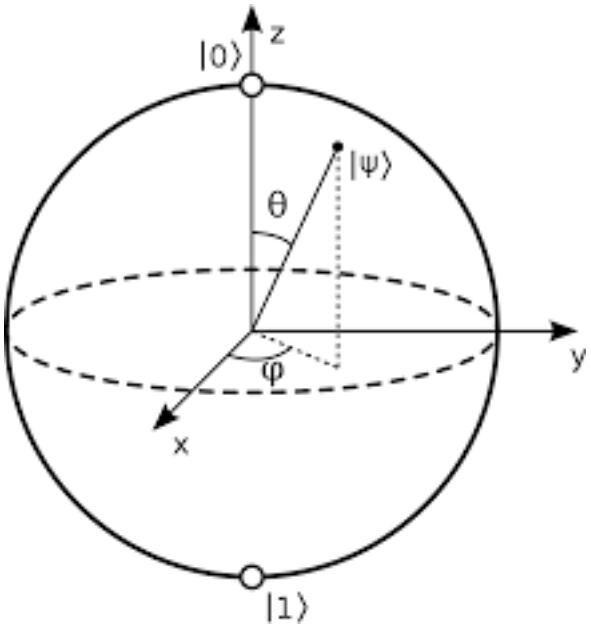

Gate's pulses

```
#see krantz page 28 eq93 to calculate the lenghts of the pulses
#for s(t) being a retangular function
#Theta(t) = - Omega * V_0 * T_s

#single qubit X/NOT gate pulse
#V0 is the amplitude
#T0 is the start of the signal
#Omega is the constant of the drive interaction given for each qubit
#wd is the qubit angular frequency
#theta is the angle desired
def X_t(t ,V0 ,T0, Omega, wd,theta):
    T_s=theta/Omega/V0
    return V0*(u_t(t-T0)-u_t(t-T0-T_s))*sin(wd*t)

#single qubit Y gate pulse
def Y_t(t ,V0 ,T0, Omega, wd,theta):
    T_s=theta/Omega/V0
    return V0*(u_t(t-T0)-u_t(t-T0-T_s))*sin(wd*t+pi/2)

#single qubit Zpi/2 gate
# H = X_pi/2 * Y_pi/2* X3pi/2
def Z_t(t ,V0 ,T0, Omega, wd, theta):
    T_sx=3*pi/2/Omega/V0
    T_sy=theta/Omega/V0
    return X_t(t ,V0 ,T0, Omega, wd, 3*pi/2)+ Y_t(t ,V0 ,T0+1.1*T_sx, Omega, wd, theta
```

```
#single qubit Hadamard gate
# H = X_pi * Y_pi/2
def Had_t(t ,V0 ,T0, Omega, wd):
    T_sx=pi/1/Omega/V0
    return X_t(t ,V0 ,T0, Omega, wd, pi)+ Y_t(t ,V0 ,T0+1.2*T_sx, Omega, wd, pi/2)
```

This function displays the expected values of the qubits:

```
 def single_qubit_graph(res, timelist):
    fig, axes = plt.subplots(1, 1, sharex=True, figsize=(10,4))

    axes.plot(timelist, np.real(expect(n1, res.states)), 'b', linewidth=2, label="qubi
    axes.plot(timelist, np.real(expect(n2, res.states)), 'g', linewidth=2, label="qubi
    axes.set_ylim(0, 1.5)
    #axes.set_xlim(0,100)

    axes.set_xlabel("Time (ns)", fontsize=16)
    axes.set_ylabel("Occupation probability", fontsize=16)
    axes.legend()

    fig.tight_layout()
```

Single qubit demonstrative operations

We prepare our initial state with Qubit 1 in a superposition to make a cat state and qubit two in $|0\rangle$

Qubit 1: $H|0\rangle = 1/\sqrt{2}|0\rangle + 1/\sqrt{2}|1\rangle$

Qubit 2: $XXHZH|0\rangle = X|1\rangle = |0\rangle$

The process on qubit two serves to demostrate the importance of the phase of the qubit. After applying Z the superposition is changed to $|Q_2\rangle = 1/\sqrt{2}|0\rangle - 1/\sqrt{2}|1\rangle$

When applying the Hadamard instead of $|0\rangle$ that we would get from the state of Qubit 1 by reapplying a Hadamard gate ,which is an involutory operator $H = H^{-1}$ and $HH|0\rangle = |0\rangle$. We get $|1\rangle$. The X operator reverses all that traformation back to $|0\rangle$ and then another X back to $|1\rangle$ and are there to show another operation as well.

```
#qubit 1 drive
def wd1_t(t, args=None):
    return Had_t(t,0.3,23,Omega1,w1)

#qubit 2 drive
def wd2_t(t, args=None):
    return Had_t(t,0.3,0,Omega2,w2) + Z_t(t,0.3,5,Omega2,w2,pi) +Had_t(t,0.3,15,Omega2


fig, axes = plt.subplots(2, 1, figsize=(10,4))
axes[0].plot(tlist, [wd1_t(t) for t in tlist], 'b', label="drive qubit1")
```

```
axes[1].plot(tlist, [wd2_t(t) for t in tlist], 'g', label="drive qubit2")
axes[0].set_ylim(-0.5,0.5)
axes[0].set_xlim(0,30)
axes[1].set_ylim(-0.5,0.5)
axes[1].set_xlim(0,30)

axes[0].set_xlabel("Time (ns)", fontsize=16)
axes[0].set_ylabel("Vd Signal Qubit 1", fontsize=16)
axes[1].set_xlabel("Time (ns)", fontsize=16)
axes[1].set_ylabel("Vd Signal Qubit 2", fontsize=16)
```

```
fig.tight_layout()
```

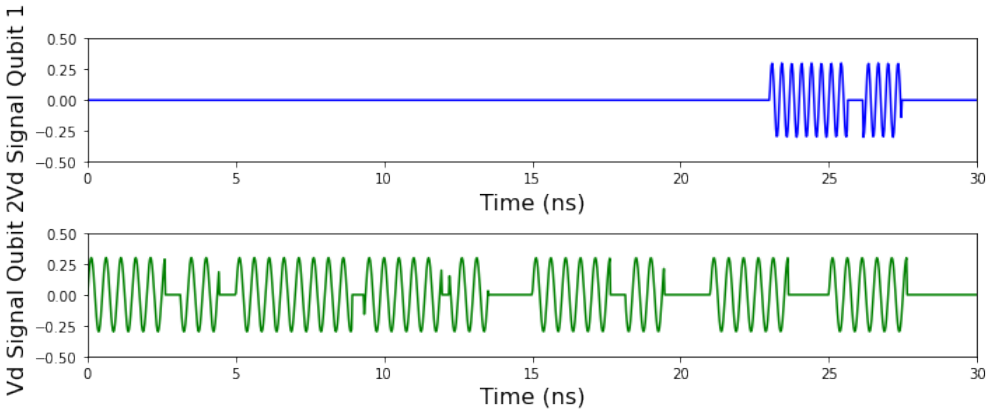

Here we can see the many pulses on each qubit as a function of time. You can notice when there is a shift in the phase of the waves in the pulses. This means the pulse switched in or out of phase with the qubit, a X type of pulse or a Y type. The qubit 1 got only a Hadamard gate made out of two pulses and the qubit 2 got many pulses comprising many gates.

Time evolution explained at: https://nbviewer.ipython.org/github/qutip/qutip-notebooks/blob/master/examples/landau-zener.ipynb

```
# method 2: a function callback that returns the coefficient for a qobj
    #H = [H0, [H1, lambda x,y: x]]
    #output = mesolve(H, psi0, tlist, c_op_list, [sm.dag() * sm], {})

#This will multiply Hd1 and Hd2 by the time dependant step functions like wd1_t during
H_t = [[Hd1, wd1_t],[Hd2, wd2_t], H1+H2]
# initial state: start with two qubits in ground state
psi0 = tensor(basis(2,0),basis(2,0))

res = mesolve(H_t, psi0, tlist[:pntperns*30], c_ops, [])

single_qubit_graph(res,tlist[:pntperns*30])
```

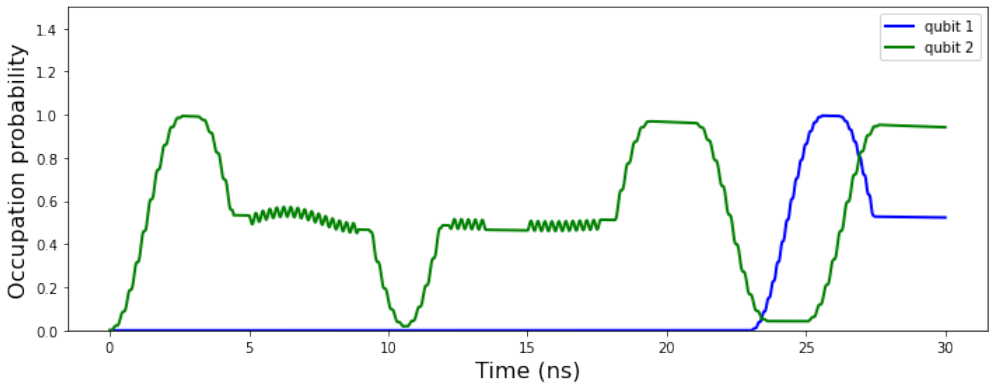

Here you can visualize the two pulses acting in qubit 1 that form the Hadamard gate, a X (from zero to 1 expected value) and a $(\pi/2)_Y$, from 1 to 0.5 expected value, a superposition.

And the pulses in qubit 2. The first Hadamard like in the Qubit 1. The Z made of three other gates, you can notice a little wiggle when there is a rotation in an axis that the qubit is parallel to (x axis here). Then the qubit goes to zero and back to the 0.5 expected value, this is the Y gate rotation. And does another longer wiggle around the 0.5 value, this is the $(3\pi/2)_X$ gate with a longer period. The last wiggle is from a X gate and it goes to 1 with another Y rotation. Then X makes it go from 1 to 0 expected qubit value.

Movement in the Bloch Sphere for the qubit 1

Here you can see it moving from the ground state $|0\rangle$ to the $|1\rangle$ state rotating around the x axis (following the right hand rule) and then 90° around the y axis to the $|1_x\rangle = \frac{1}{\sqrt{2}}|0\rangle + \frac{1}{\sqrt{2}}|1\rangle$ state.

```
#creates the time dependant unitaries vector to cancel the precession
Ud_vec=[]
for t in tlist[:pntperns*30]:
    Ud=sz1*t*w1*complex(0,-1)/2
    Ud_vec.append(Ud.expm())

#multiplies each state vector by the corresponding Unitary in time
bloch_data=[]
for index in range(len(res.states)):
    bloch_data.append(Ud_vec[index]*res.states[index])

#Pauli operators
ex=tensor(sigmax(),qeye(2))
ey=tensor(sigmay(),qeye(2))
ez=tensor(sigmaz(),qeye(2))

#lists of expected values that are the coordinates of the points in the bloch sphere
x_list=expect(ex,bloch_data)
y_list= expect(ey,bloch_data)
```

```
z_list=expect(ez,bloch_data)


b = Bloch()
## add data points from expectation values ##
b.add_points([
            x_list,
            -y_list,
            z_list
             ], meth='l')


b.zlpos = [1.1,-1.2]

b.show()
```

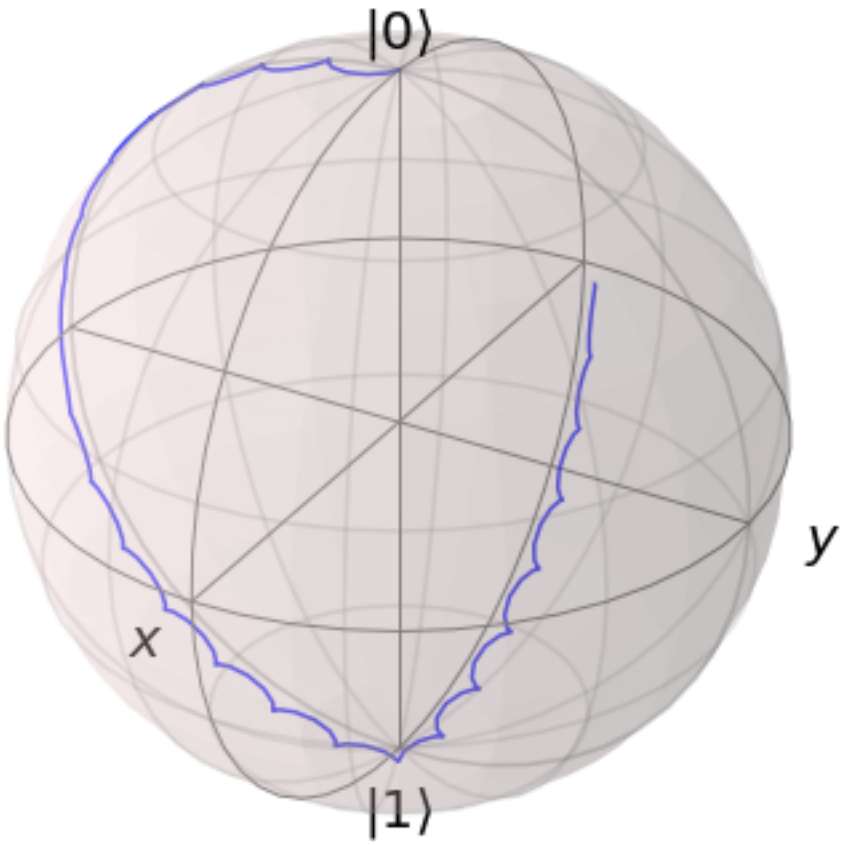

Movement in the Bloch Sphere for the qubit 2

Since there are many gates applied on this qubit it takes more effort to decipher the path it took. But you can notice for example the wiggle the qubit does when you apply a x rotation when it's already at the x axis. I made each gate in different colors (the tow last Xs are the same color). The first Hadamard is blue, the Z gate is red, the second Hadamard is green and the two Xs on the end are orange making a 360° lap on the sphere.

```
#creates the time dependant unitaries vector to cancel the precession
Ud_vec=[]
for t in tlist[:pntperns*30]:
    Ud=sz2*t*w2*complex(0,-1)/2
    Ud_vec.append(Ud.expm())

#multiplies each state vector by the corresponding Unitary in time
bloch_data=[]
for index in range(len(res.states)):
    bloch_data.append(Ud_vec[index]*res.states[index])

#Pauli operators
ex=tensor(qeye(2), sigmax())
ey=tensor(qeye(2), sigmay())
ez=tensor(qeye(2), sigmaz())

#lists of expected values that are the coordinates of the points in the bloch sphere
x_list=expect(ex,bloch_data)
y_list= expect(ey,bloch_data)
z_list=expect(ez,bloch_data)


b = Bloch()
## add data points from expectation values ##
b.add_points([
            x_list[:5*pntperns],
            -y_list[:5*pntperns],
            z_list[:5*pntperns]
             ], meth='l')

b.add_points([
            x_list[5*pntperns:15*pntperns],
            -y_list[5*pntperns:15*pntperns],
            z_list[5*pntperns:15*pntperns]
             ], meth='l')

b.add_points([
            x_list[15*pntperns:20*pntperns],
            -y_list[15*pntperns:20*pntperns],
```

```
            z_list[15*pntperns:20*pntperns]
             ], meth='l')

b.add_points([
            x_list[20*pntperns:30*pntperns],
            -y_list[20*pntperns:30*pntperns],
            z_list[20*pntperns:30*pntperns]
             ], meth='l')


b.zlpos = [1.1,-1.2]

b.show()
```

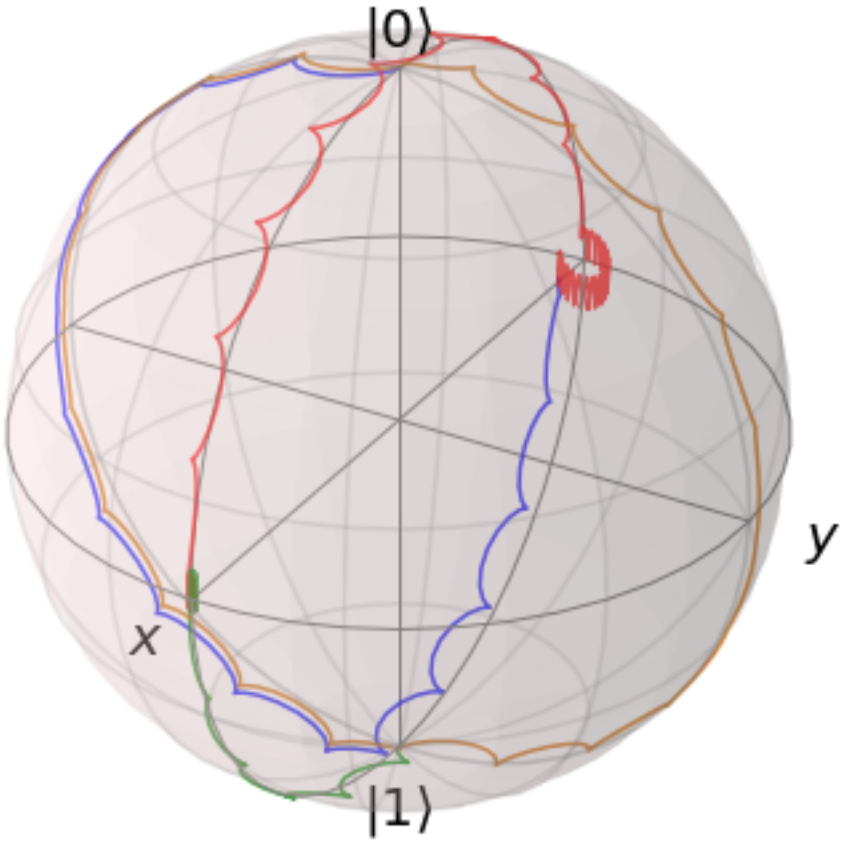

The CNOT gate

The CNOT gate can be build from two iSWAP gates and single qubit gates. Image from krantz page 32 IV-E-2 shown below:

```
Image(filename='images/notebook-cnot.png')
```

2. *Applications of the iSWAP gate*

The iSWAP cannot generate a CNOT gate by itself. Rather, to implement a CNOT gate requires stringing together two iSWAPs and several single qubit gates[217],

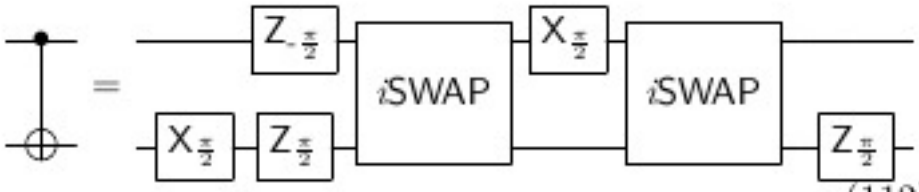

(112)

As evident from Eq. (112), the iSWAP gate in general needs to be used twice to generate a single CNOT, leading to a significant overhead when compiling CNOT–dense

Initial single gates

Here we do the initial single qubit gates before the first iSWAP

```
# initial state: use last state of the last simulation
psi1 = res.states[-1]
```

```
psi1
```

Quantum object: dims = [[2, 2], [2, 2]], shape = (4, 4), type = oper, isherm = True

$$\begin{pmatrix} 0.028 & (0.001-0.006j) & (-0.028+0.004j) & (-3.611\times10^{-04}+0.006j) \\ (0.001+0.006j) & 0.449 & (-0.002-0.006j) & (-0.456+0.068j) \\ (-0.028-0.004j) & (-0.002+0.006j) & 0.030 & (0.001-0.006j) \\ (-3.611\times10^{-04}-0.006j) & (-0.456-0.068j) & (0.001+0.006j) & 0.493 \end{pmatrix}$$

```
#qubit 1 drive
def wd1_t(t, args=None):
    return Z_t(t,0.3,2,Omega1,w1,pi/2)

#qubit 2 drive
def wd2_t(t, args=None):
    return X_t(t,0.3,0,Omega2,w2,pi/2) + Z_t(t,0.3,3,Omega2,w2,pi/2)


H_t = [[Hd1, wd1_t],[Hd2, wd2_t], H1+H2]
# initial state: start with two qubits in ground state
res = mesolve(H_t, psi1, tlist[:pntperns*11], c_ops, [])
```

```
single_qubit_graph(res,tlist[:pntperns*11])
```

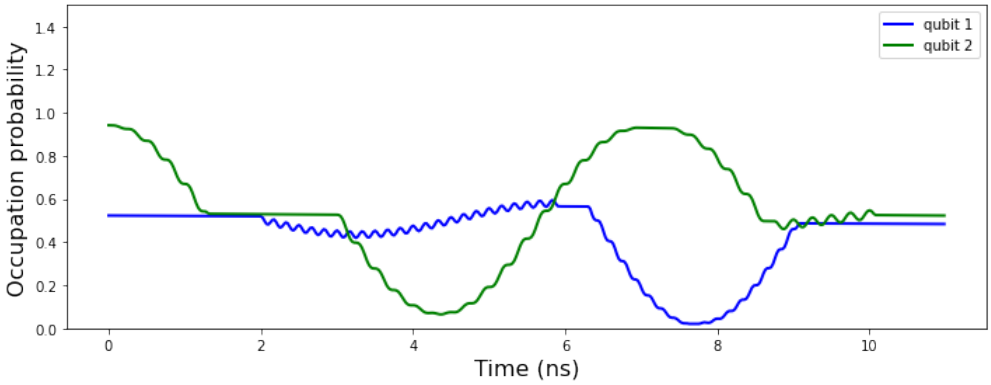

The iSWAP gate

A 2-qubit XX+YY interaction. This is a Clifford and symmetric gate. Its action is to swap two qubit states and phase the |01⟩ and |10⟩ amplitudes by i.

It's made by doing a resonance of both qubits for a determined period. In the simulation I will just adjust the frequency of a qubit to match the other. But in practice this can be made by adjusting a magnetic flux going through the two qubits so that the frequency(dependant on the flux) adjusts to a value where both are equal. The period for the iSWAP is given by the formula:

$\tau = \frac{\pi}{2g}$

I will implement a special Hamiltonian for it to be used again later.

```
# initial state: use last state of the last simulation
psi2 = res.states[-1]
```

```
psi2
```

Quantum object: dims = [[2, 2], [2, 2]], shape = (4, 4), type = oper, isherm = True

$$\begin{pmatrix} 0.246 & (-0.216+0.032j) & (-0.111-0.201j) & (0.123+0.162j) \\ (-0.216-0.032j) & 0.270 & (0.071+0.191j) & (-0.122-0.221j) \\ (-0.111+0.201j) & (0.071-0.191j) & 0.231 & (-0.202+0.030j) \\ (0.123-0.162j) & (-0.122+0.221j) & (-0.202-0.030j) & 0.253 \end{pmatrix}$$

```
# resonant iSWAP gate 2 qubits
T0 = 2
T_gate =pi/2/g
```

```
#qubit energy is changed to enter ressonance with other qubit in interval [T_0, T_0+T_
def w1_t(t, args=None):
    return 1 + (w2/w1-1)*(u_t(t-T0)-u_t(t-T0-T_gate))

times=tlist[:pntperns*30]
```

```
#This will multiply Hc H1 and H2 by the time dependant step functions like wc_t during
H_t_iSWAP = [ [H1, w1_t], Hqq+H2]

res = mesolve(H_t_iSWAP, psi2, times, c_ops, [])

fig, axes = plt.subplots(2, 1, sharex=True, figsize=(10,8))

axes[0].plot(times, [w1_t(t)*w1 for t in times], 'b', label="qubit1")
axes[0].plot(times, [w2 for t in times], 'g', label="qubit2")
#axes.set_ylim(-0.6,0.6)
#axes.set_xlim(0,100)

axes[0].set_ylabel("Energy (GHz)", fontsize=16)
axes[0].set_xlabel("Time (ns)", fontsize=16)
axes[0].legend()

axes[0].legend()

axes[1].plot(times, np.real(expect(n1, res.states)), 'b', linewidth=2, label="qubit 1"
axes[1].plot(times, np.real(expect(n2, res.states)), 'g', linewidth=2, label="qubit 2"
axes[1].set_ylim(0, 1.5)
#axes[1].set_xlim(0,20)

axes[1].set_xlabel("Time (ns)", fontsize=16)
axes[1].set_ylabel("Occupation probability", fontsize=16)
axes[1].legend()


fig.tight_layout()
```

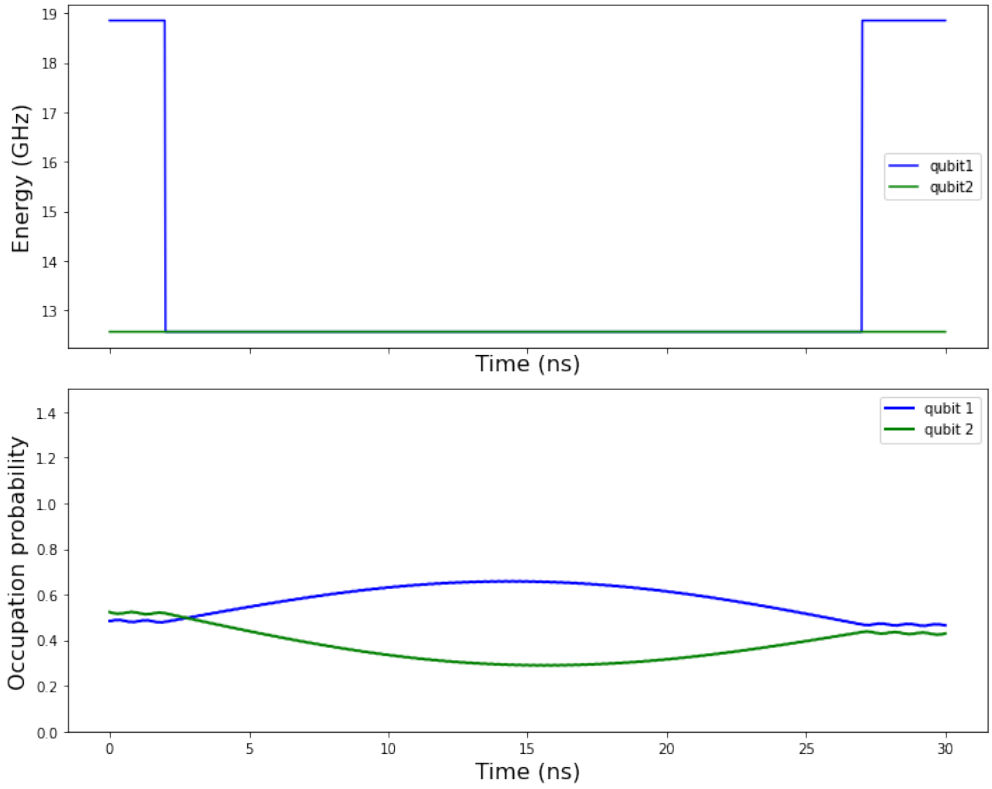

You can see in the energy graph how a resonance is necessary for the interaction visible in the occupation probability graph where the cavity and qubit exchange their states. First with qubit 1 and then with qubit 2.

$X_\pi/2$ in between gate

```
# initial state: use last state of the last simulation
psi3 = res.states[-1]
```

```
psi3
```

Quantum object: dims = [[2, 2], [2, 2]], shape = (4, 4), type = oper, isherm = True

$$\begin{pmatrix} 0.303 & (0.175-0.119j) & (-0.060-0.207j) & (0.133+0.120j) \\ (0.175+0.119j) & 0.232 & (0.056-0.177j) & (0.044+0.165j) \\ (-0.060+0.207j) & (0.056+0.177j) & 0.267 & (-0.177+0.115j) \\ (0.133-0.120j) & (0.044-0.165j) & (-0.177-0.115j) & 0.198 \end{pmatrix}$$

```
#qubit 1 drive
def wd1_t(t, args=None):
    return X_t(t,0.3,5,Omega1,w1,pi/2)

#qubit 2 drive
def wd2_t(t, args=None):
    return 0
```

```
H_t = [[Hd1, wd1_t],[Hd2, wd2_t], H1+H2]

res = mesolve(H_t, psi3, tlist[:pntperns*7], c_ops, [])

single_qubit_graph(res,tlist[:pntperns*7])
```

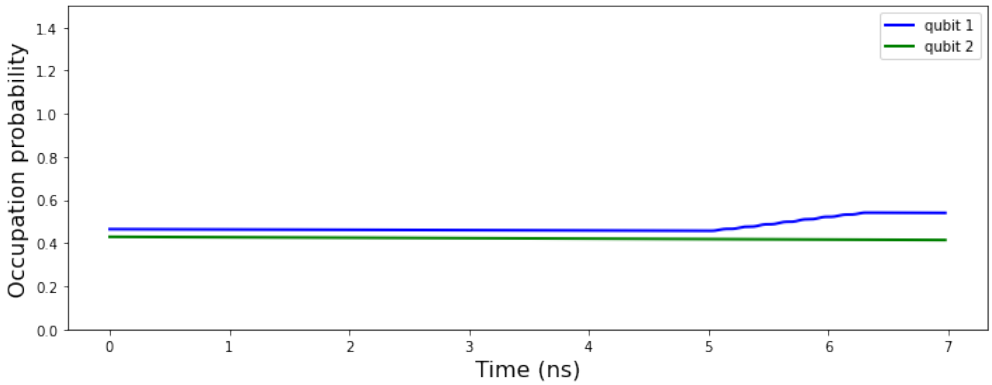

Second iSWAP

```
# initial state: use last state of the last simulation
psi4 = res.states[-1]

psi4
```

Quantum object: dims = [[2, 2], [2, 2]], shape = (4, 4), type = oper, isherm = True

$$\begin{pmatrix} 0.093 & (-0.036-0.023j) & (-0.055-0.001j) & (-0.030-0.008j) \\ (-0.036+0.023j) & 0.366 & (0.180-0.330j) & (0.026-0.034j) \\ (-0.055+0.001j) & (0.180+0.330j) & 0.492 & (0.033+0.019j) \\ (-0.030+0.008j) & (0.026+0.034j) & (0.033-0.019j) & 0.048 \end{pmatrix}$$

```
res = mesolve(H_t_iSWAP, psi4, times, c_ops, [])

fig, axes = plt.subplots(1, 1, sharex=True, figsize=(10,4))


axes.plot(times, np.real(expect(n1, res.states)), 'b', linewidth=2, label="qubit 1")
axes.plot(times, np.real(expect(n2, res.states)), 'g', linewidth=2, label="qubit 2")
axes.set_ylim(0, 1.5)
#axes[1].set_xlim(0,20)

axes.set_xlabel("Time (ns)", fontsize=16)
axes.set_ylabel("Occupation probability", fontsize=16)
axes.legend()


fig.tight_layout()
```

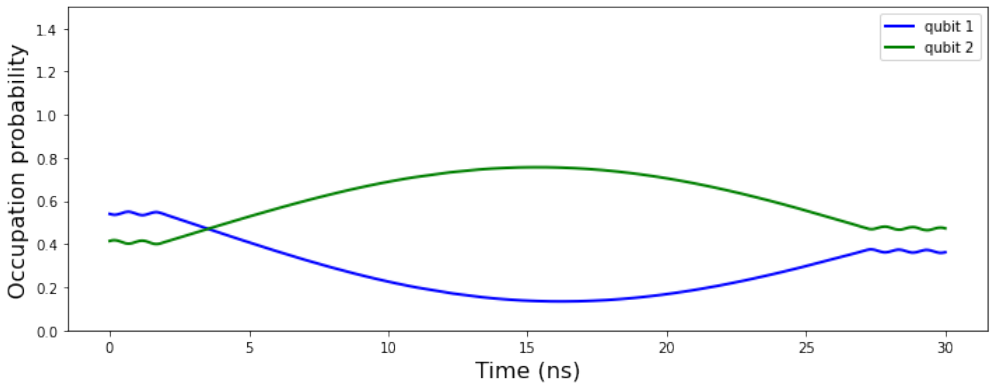

$Z_\pi/2$ final gate

```
# initial state: use last state of the last simulation
psi5 = res.states[-1]

#qubit 1 drive
def wd1_t(t, args=None):
    return 0

#qubit 2 drive
def wd2_t(t, args=None):
    return Z_t(t,0.3,1,Omega2,w2,pi/2)

H_t = [[Hd1, wd1_t],[Hd2, wd2_t], H1+H2]

res = mesolve(H_t, psi5, tlist[:pntperns*10], c_ops, [])

single_qubit_graph(res,tlist[:pntperns*10])
```

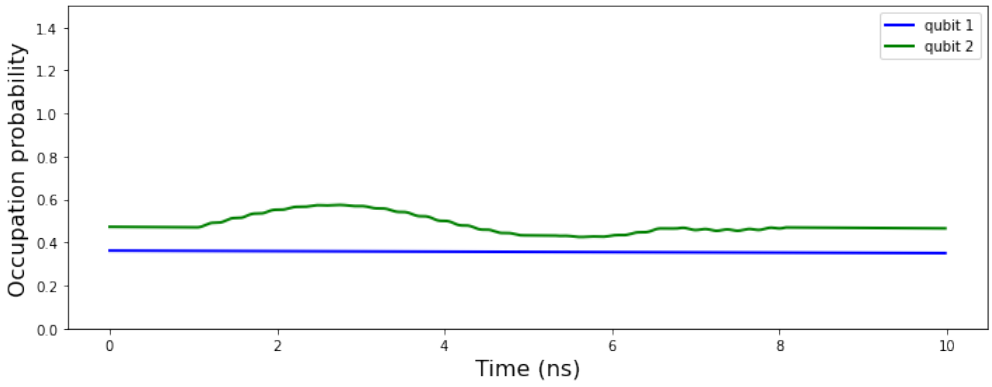


```
final=res.states[-1]
```

Final answer density matrix of the qubits

The answer expected for the problem was the state vector:

$|\Psi\rangle = \frac{1}{\sqrt{2}}|01\rangle + \frac{1}{\sqrt{2}}|10\rangle$

or the density matrix:

$\rho = 0.5|01\rangle\langle 01| + 0.5|10\rangle\langle 10|$

Because we did a CNOT with the controller qubit 1 at a Hadamard superposition $(\frac{\sqrt{2}}{2}|0\rangle + \frac{\sqrt{2}}{2}|1\rangle)$ and the controlled qubit 2 at $|1\rangle$

$CNOT_{1,2}X_2H_1|0_20_1\rangle = CNOT_{1,2}|1_2\rangle(\frac{1}{\sqrt{2}}|0_1\rangle + \frac{1}{\sqrt{2}}|1_1\rangle) = \frac{1}{\sqrt{2}}|01\rangle + \frac{1}{\sqrt{2}}|10\rangle$

The density matrix above ρ is made explicit below for a better comparison:

```
0.5*(tensor(basis(2,1),basis(2,0))*tensor(basis(2,1),basis(2,0)).dag()+tensor(basis(2
```

Quantum object: dims = [[2, 2], [2, 2]], shape = (4, 4), type = oper, isherm = True

$$\begin{pmatrix} 0.0 & 0.0 & 0.0 & 0.0 \\ 0.0 & 0.500 & 0.0 & 0.0 \\ 0.0 & 0.0 & 0.500 & 0.0 \\ 0.0 & 0.0 & 0.0 & 0.0 \end{pmatrix}$$

$|0_10_2\rangle|0_11_2\rangle|1_10_2\rangle|1_11_2\rangle$

```
#answer with dissipation
final
```

Quantum object: dims = [[2, 2], [2, 2]], shape = (4, 4), type = oper, isherm = True

$$\begin{pmatrix} 0.222 & (0.046 - 0.018j) & (3.144 \times 10^{-04} - 0.046j) & (-0.012 - 0.021j) \\ (0.046 + 0.018j) & 0.428 & (0.244 - 0.194j) & (0.006 - 0.027j) \\ (3.144 \times 10^{-04} + 0.046j) & (0.244 + 0.194j) & 0.312 & (0.013 - 0.028j) \\ (-0.012 + 0.021j) & (0.006 + 0.027j) & (0.013 + 0.028j) & 0.038 \end{pmatrix}$$

With dissipation we get this density matrix which has a similiarity to the expect answer but has some probability on the $|00\rangle$ state because of the qubits' relaxation to the $|0\rangle$ state.

```
#answer without dissipation
final*final.dag()
```

Quantum object: dims = [[2, 2], [2, 2]], shape = (4, 4), type = oper, isherm = True

$$\begin{pmatrix} 0.010 & (0.032 - 0.062j) & (-0.013 - 0.068j) & (-0.004 - 0.007j) \\ (0.032 + 0.062j) & 0.495 & (0.385 - 0.305j) & (0.032 - 0.049j) \\ (-0.013 + 0.068j) & (0.385 + 0.305j) & 0.488 & (0.055 - 0.018j) \\ (-0.004 + 0.007j) & (0.032 + 0.049j) & (0.055 + 0.018j) & 0.007 \end{pmatrix}$$

Without dissipation we get a matrix that is quite similar to the final answer. Much more so than with dissipation for obvious reasons.

Qutip Jupyter notebook to find the interaction factor between two qubits

This section is a jupyter notebook that can be found on Github (link)

Here we simulate two qubits and vary the frequency of one of them to measure the amount of interaction it has with one another. In this case with a iSWAP gate like used before. Then we vary the time they interact and conduct a measurement from whose period of variation of the state transfer we can find g the interaction factor. This is supposed to emulate a common process of calibration of this factor in a real quantum computer.

Simulating the calibration of the g interaction factor between two qubits

In this notebook we will simulate two qubits that are simulated with an interaction for values close to and in their resonance to emulate the process used in real quantum computers to calibrate the factor of interaction between them. This factor is used to determine the lenght of pulses used in two qubit gates like the iSWAP.

The process starts with the qubit 1 at the excited state $|1\rangle$ (in real life using a π pulse on the ground state). And the other qubit (2) at the ground state $|0\rangle$. Then we use (for example a different magnetic flux on the qubits) to change the energy/angular frequency of qubit 1 and map it across many energies around the energy of qubit 2. Then we do many different time intervals in these states of an altered energy and measure the value on qubit 2 many times. Getting a probability of it being in the excited state (sucessful swap with qubit 1). Mapping both the time intervals and the energies we can infer the g factor of interaction from the peaks in our map.

```
%matplotlib inline

from qutip import *

from math import *
import matplotlib.pyplot as plt
import numpy as np


import timeit
```

Constants

```
w1 = 3.0 * 2 * pi #qubit 1 angular freq
w2 = 2.0 * 2 * pi #qubit 2 angular freq

g = 0.01 * 2 * pi
```

```
width = 0.5

time_interval=100
points=50
tlist = np.linspace(0, time_interval, points)

#rotating wave approximation
use_rwa= False
```

Value of g used

```
g
```

```
0.06283185307179587
```

Operators

```
sm1 = tensor(destroy(2), qeye(2))

sz1 = tensor(sigmaz(), qeye(2))
sy1 = tensor(sigmay(), qeye(2))
sx1 = tensor(sigmax(), qeye(2))
n1 = sm1.dag() * sm1

# operators for qubit 2
sm2 = tensor(qeye(2), destroy(2))

sz2 = tensor(qeye(2), sigmaz())
sy2 = tensor(qeye(2), sigmay())
sx2 = tensor(qeye(2), sigmax())
n2 = sm2.dag() * sm2
```

Hamiltonian

```
# Hamiltonian using QuTiP

#qubits
H1 = - 0.5 * sz1 * w1
H2 = - 0.5 * sz2 * w2

#Qubit coupling hamiltonian
# Hamiltonian
if use_rwa:
    Hqq = -g/2 * (sx1*sx2+sy1*xy2)
else:
    Hqq = -g * (sm1.dag() - sm1) * ( sm2.dag()-sm2)
```

```
#unitary step function
def u_t(t):
    return 1*(t > 0)

def simulate(T0,T_gate,w,tlist):

    start = timeit.default_timer()

    #Your statements here

    psi = tensor(basis(2,1),basis(2,0))

    def w1_t(t, args=None):
                    return 1 + (w/w1-1)*(u_t(t-T0)-u_t(t-T0-T_gate))

    #This will multiply H1 and H2 by the time dependant step functions like w1_t duri
    H_t = [ [H1, w1_t], H2+Hqq]
    #result of the simulation with a list of state vectors
    res = mesolve(H_t, psi, tlist, [], [])
    stop = timeit.default_timer()
   # print('Time: ', stop - start)
    return res

def graph_simu(res):
    fig, axes = plt.subplots(1, 1, sharex=True, figsize=(10,4))

    axes.plot(tlist, np.real(expect(n1, res.states)), 'b', linewidth=2, label="qubit
    axes.plot(tlist, np.real(expect(n2, res.states)), 'g', linewidth=2, label="qubit
    axes.set_ylim(0, 1)
    #axes[1].set_xlim(0,20)

    axes.set_xlabel("Time (ns)", fontsize=16)
    axes.set_ylabel("Occupation probability", fontsize=16)
    axes.legend()


    fig.tight_layout()
```

Simulations of the expected value for both qubits when qubit 1 is approximated to the qubit 2 frequency at various intervals.

In real life we wouldn't be able to obtain these graphs easily because we'd need to measure the expected value by many measurements for each time in the x axis for both qubits. But since this is a simulation we can see than to better understand the system. Here I varied the energy of the qubit 1 around the w2 value of the energy of qubit 2. The further we go from it, the weaker is the swap/interaction. Positive and negative differences from the value of qubit 2 are symetrical.

```
graph_simu(simulate(10,80,w2,tlist))
```

```
Time:  0.02499551698565483
```

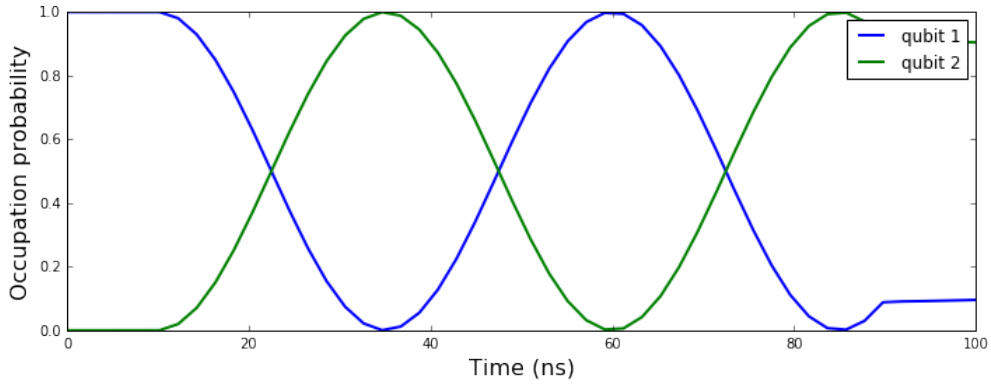


```
graph_simu(simulate(10,80,w2+0.02,tlist))
```

```
Time:  0.02205941453576088
```

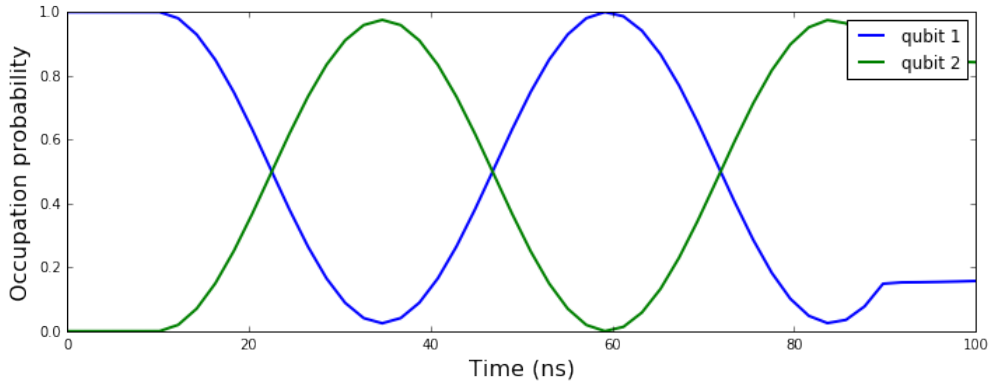


```
graph_simu(simulate(10,80,w2+0.04,tlist))
```

```
Time:  0.021794598549604416
```

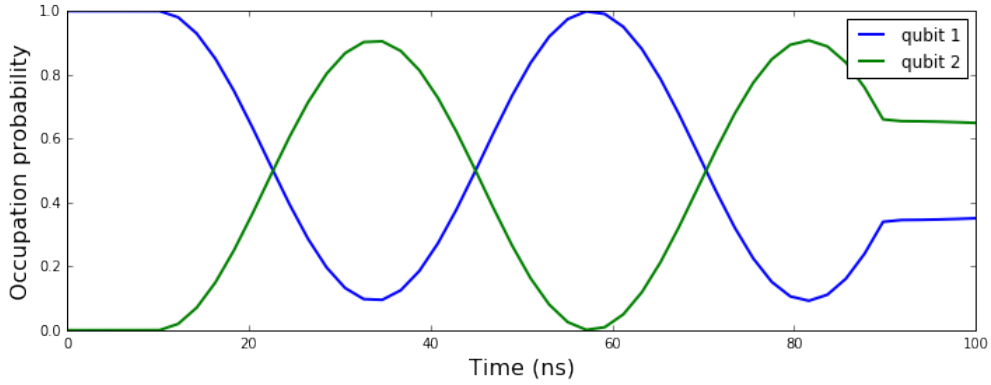


```
graph_simu(simulate(10,80,w2-0.04,tlist))
```

```
Time:  0.02172275260090828
```

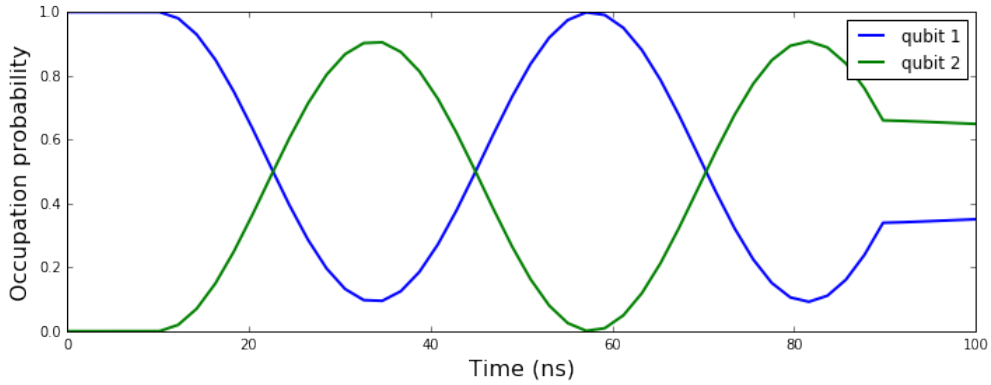


```
graph_simu(simulate(10,80,w2+0.08,tlist))
```

```
Time:  0.0216141939163208
```

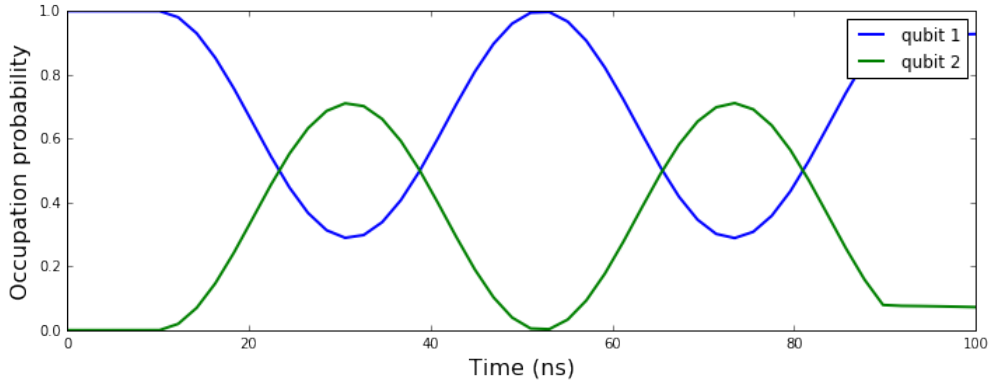


```
graph_simu(simulate(10,80,w2-0.08,tlist))
```

```
Time:  0.022494543343782425
```

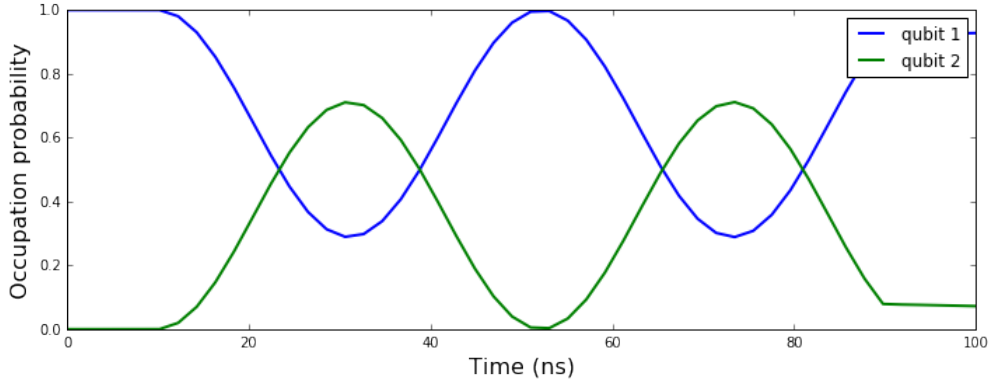


```
graph_simu(simulate(10,80,w2+0.2,tlist))
```

```
Time:  0.023160740733146667
```

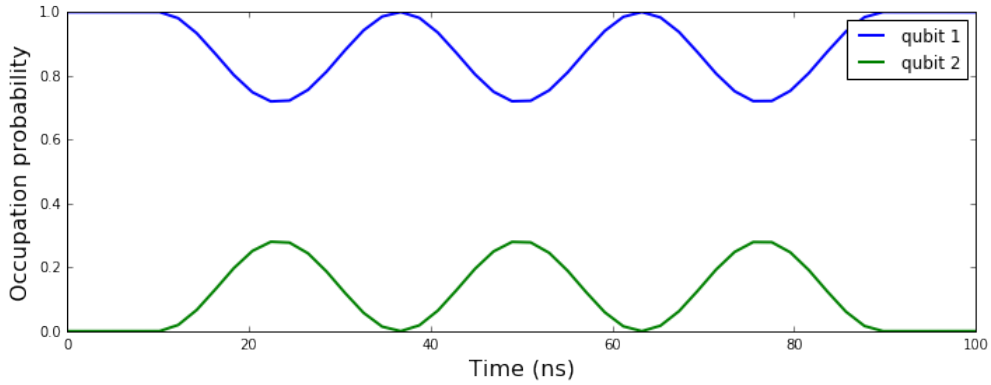


```
graph_simu(simulate(10,80,w2+0.3,tlist))
```

```
Time:  0.023189201951026917
```

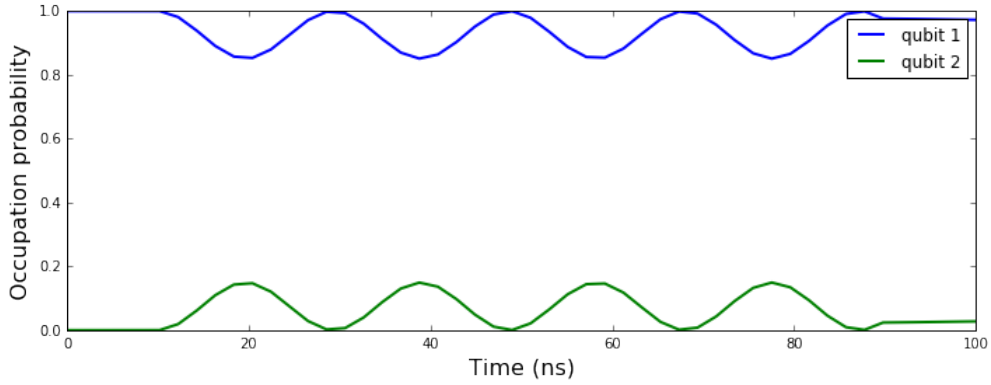


```
graph_simu(simulate(10,80,w2+0.5,tlist))
```

```
Time:  0.024360783398151398
```

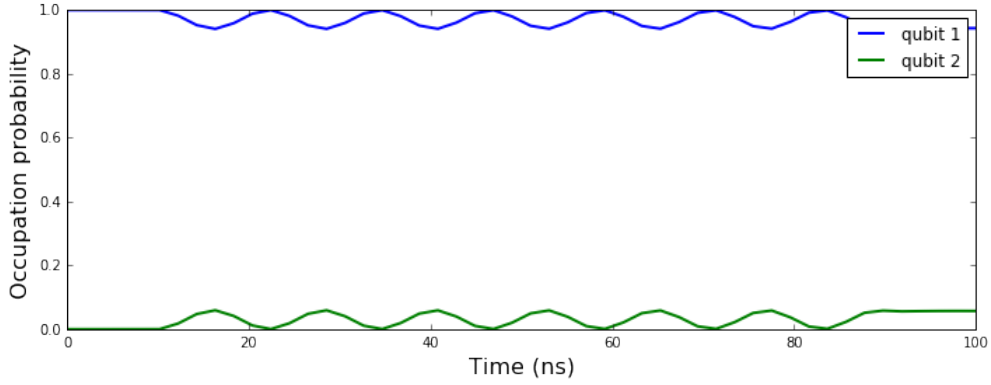


```
graph_simu(simulate(10,80,w2+2,tlist))
```

```
Time:  0.02978280931711197
```

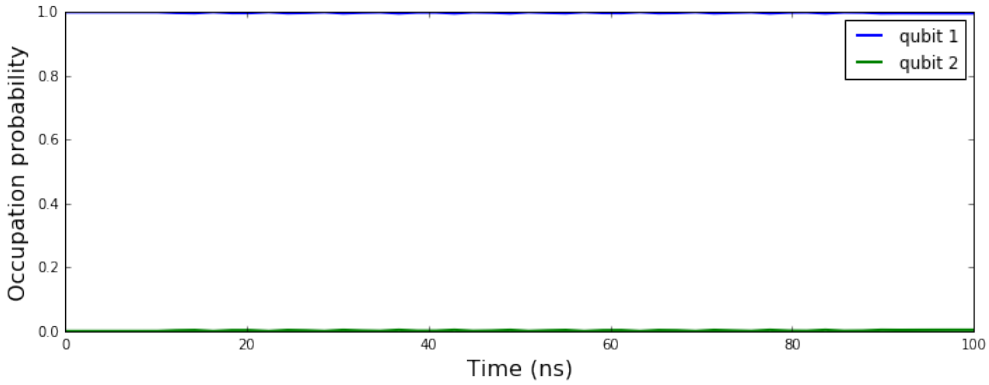

Mapping of the interaction

Here we will finally map the energies and the time intervals we applied the change in energy and produce a graph to visualize it. Then we will estimate the value of g from the graph.

```
def measure(expected):
    if np.random.random()<=expected:
        return 1
    else:
        return 0


time_interval=100
points=50
pntperns=ceil(points/time_interval)

intervals = np.linspace(1, time_interval, ceil(points/2))
energies = np.linspace(w2-2,w2+2 , ceil(points/2))

measurements=20

matrix=[]
for w in energies:
    vector_times=[]
    for T_gate in intervals:
        average=0
        for i in range(measurements):

            #shrinks simulation for efficiency
            times = np.linspace(0, T_gate, points)

            #Measure last value in the simulation and add to average
            res=simulate(0,T_gate,w,times)
            result=measure((expect(n2, res.states[-1])))

            average+=result
```

```
            #makes a vector of the probabilities obtained for each time interval
            vector_times.append(average/measurements)

        #makes a matrix with the vectors of time intervals' probabilies for each flux
        matrix.append(vector_times)

Z = np.array(matrix).T.tolist()
y = intervals
x =  energies

fig, ax = plt.subplots()
im=ax.pcolormesh(x, y, Z)

ax.set_xlabel("Angular frequency", fontsize=16)
ax.set_ylabel("Interval time (ns)", fontsize=16)

fig.colorbar(im, ax=ax)
plt.show()
```

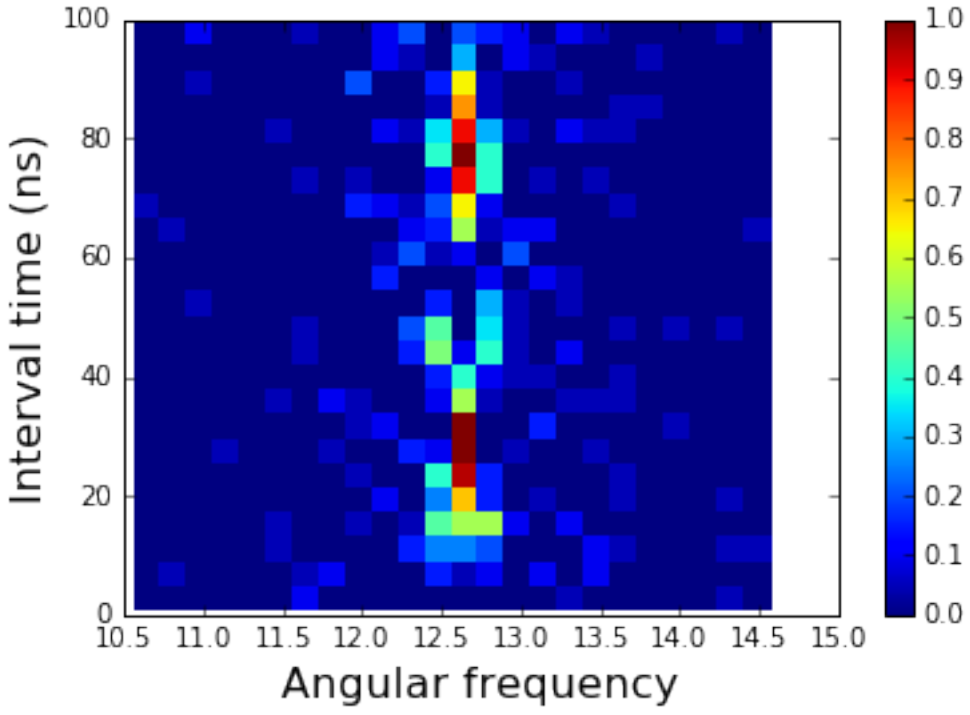

Looking at the graph and given that the period of the iSWAP gate (where the probability peaks) is $\frac{\pi}{2g}$ we get roughly that

$$g = \frac{\pi}{2t_{peak}} = \frac{\pi}{2 \cdot 30} = 0.05236$$

Which given the real g used in the simulation and that the resolution we used is very low:

```
g
```

```
0.06283185307179587
```

It is a good result for our didactical goals. Although for a real calibration it wouldn't really be appropriate.

Qutip Jupyter notebook to simulate a measurement

This section is a jupyter notebook that can be found on Github (link) In the last notebook of the simulations we emulate the process of conducing a measurement through a cavity. For that we drive the cavity with a cosine wave and read the reflected/transmitted back wave with the a operator expected value for the cavity. Different states of the qubit will result in waves with different frequency as explained further in the notebook.

Doing a measurement on a Qubit through a cavity

This notebook will show how a measurement is made on a qubit trough a signal sent through the cavity. Depending on the state of the qubit the cavity's resonance frequency will change a small amount and the output of this signal we sent to the cavity will change. This is explained by the Hamiltonian of the interaction. In the dispersive regime we can approximate the Hamiltonian to:

$$H = \omega_r a^\dagger a - \frac{1}{2}\omega_q \sigma_z + \chi(a^\dagger a + 1/2)\sigma_z$$

And rearrange it to:

$$H = a^\dagger a(\omega_r + \chi\sigma_z) - \frac{1}{2}\omega_q \sigma_z + \chi(1/2)\sigma_z$$

Where $\chi = g^2/\Delta$ and $\Delta = |wc - w1|$. We can get from this an intuition that the state of the qubit expressed by σ_z will change the angular frequency $(\omega_r + \chi\sigma_z)$ of the cavity (by plus or minus χ) and we will measure a different amount of photons depending on the state of the qubit. Following the principles of quantum mechanics this will of course colapse the qubit's wave function to the measured value.

For the simulation we use a Jaynes-Cumming Hamiltonian modified to have a drive in the cavity:

$H = \hbar\omega_r a^\dagger a + A\cos(\omega_d t + \phi_0)(a + a^\dagger) - \frac{1}{2}\hbar\omega_c\sigma_z + g(a^\dagger + a)(\sigma_- + \sigma_+)$

Where $ A \cos(\omega_dt + \phi_0)$ is the drive in the cavity.Rewritten as:

$H = \hbar\omega_r a^\dagger a + (Ae^{-i\omega_d t} + A^* e^{+i\omega_d t})(a + a^\dagger) - \frac{1}{2}\hbar\omega_c\sigma_z + g(a^\dagger + a)(\sigma_- + \sigma_+)$

Then we use a unitary transformation at the Hamiltonian:

$U = exp(i\omega_d a^\dagger a t)$

And the rotating wave approximation to elimitate fast rotating terms getting the hamiltonian used:

$H = (\omega_c - \omega)a^\dagger a + A(a + a^\dagger) - \frac{1}{2}(\omega_q - \omega)\sigma_z + g(a^\dagger + a)(\sigma_- + \sigma_+)$

Where $\omega = g^2/|\omega_c - \omega_d|$

This process for a single cavity can be seen with more details at:

https://nbviewer.org/github/jrjohansson/sympsi-notebooks/blob/master/lecture-sympsi-resonator.ipynb

```
%matplotlib inline

from qutip import *
from math import *

import matplotlib.pyplot as plt
import numpy as np

N = 10

wc = 4.5 * 2 * pi #cavity angular freq
w1 = 4 * 2 * pi #qubit 1 angular freq


g1 = 0.1 * 2 * pi

Omega1=4

chi=g1**2/abs(wc-w1)

tlist = np.linspace(0, 20, 1600)

width = 0.5

#rotating wave approximation
use_rwa= False

w=chi
w

0.1256637061435917

# cavity operators
a = tensor(destroy(N), qeye(2))
n = a.dag() * a

# operators for qubit 1
sm1 = tensor(qeye(N), destroy(2))
sz1 = tensor(qeye(N), sigmaz())
sy1 = tensor(qeye(N), sigmay())
sx1 = tensor(qeye(N), sigmax())
n1 = sm1.dag() * sm1
```

```
# Hamiltonian using QuTiP
#cavity
Hc = a.dag() * a * (wc-w)
#qubits
H1 = - 0.5 * sz1 * (w1-w)

#cavity drive
Hdc = (a.dag() + a )

#2*sx
#s+=[[0,1],[0,0]]
#s-=s+.dag()

#qubit drive
Hd1=Omega1*sy1


#Cavity-qubit coupling hamiltonians
# Hamiltonian
if use_rwa:
    Hc1 = g1 * (a.dag() * sm1 + a * sm1.dag())
else:
    Hc1 = g1 * (a.dag() + a) * (sm1 + sm1.dag())

#unitary step function
def u_t(t):
    return 1*(t > 0)

#qubit 1 drive
#A = (1/3)*0.0002# field aplitude
def A_t(t, args=None):
    TA1=1
    T_As=10
    Amp=1
    return Amp*(u_t(t-TA1)-u_t(t-TA1-T_As))
#+ Amp*(u_t(t-TA2)-u_t(t-TA2-T_As)))

fig, axes = plt.subplots(1, 1, figsize=(10,4))

axes.plot(tlist, [A_t(t) for t in tlist], 'r', label="drive cavity")
axes.set_ylim(-0.2,1.2)
axes.set_xlim(0,20)
axes.set_xlabel("Time (ns)", fontsize=16)
axes.set_ylabel("Vd Signal Cavity", fontsize=16)



fig.tight_layout()
```

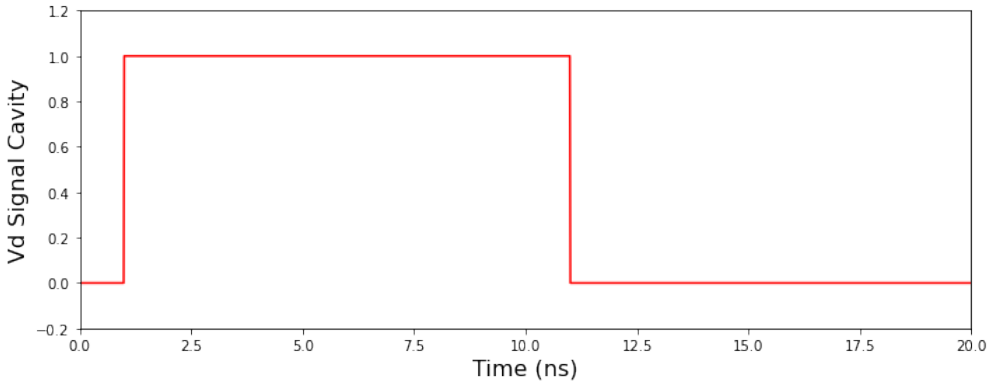


```
# method 2: a function callback that returns the coefficient for a qobj
    #H = [H0, [H1, lambda x,y: x]]
    #output = mesolve(H, psi0, tlist, c_op_list, [sm.dag() * sm], {})

#This will multiply Hd1 and Hd2 by the time dependant step functions like wd1_t during
H_t = [[Hdc,A_t], Hc+H1+Hc1]
# initial state: start with two qubits in ground state
psi0 = tensor(basis(N,0),basis(2,0))
psi1 = tensor(basis(N,0),basis(2,1))
res0 = mesolve(H_t, psi0, tlist, [], [])
res1 = mesolve(H_t, psi1, tlist, [], [])
```

Then we graph the expected value of the operator a which is the photon output of the cavity and the value we would measure coming reflected from it in a real situation.

```
def single_qubit_graph(res1, res0):
    fig, axes = plt.subplots(1, 1, sharex=True, figsize=(10,4))

    #axes.plot(tlist, np.real(expect(n1, res.states)), 'b', linewidth=2, label="qubit 1
    #axes.plot(tlist, np.abs(expect(n, res.states)), 'r', linewidth=2, label="cavity")
    axes.plot(tlist, np.abs(expect(a, res1.states)), 'b', linewidth=2, label="qubit in
    axes.plot(tlist, np.abs(expect(a, res0.states)), 'r', linewidth=2, label="qubit in
   #
    #axes.plot(tlist, np.imag(expect(a, res.states)), 'g', linewidth=2, label="cavity")
   # axes.set_ylim(0, 1.5)
    #axes.set_xlim(1,10)

    axes.set_xlabel("Time (ns)", fontsize=16)
    axes.set_ylabel("Expected value of a", fontsize=16)
    axes.legend()

    fig.tight_layout()

single_qubit_graph(res1, res0)
```

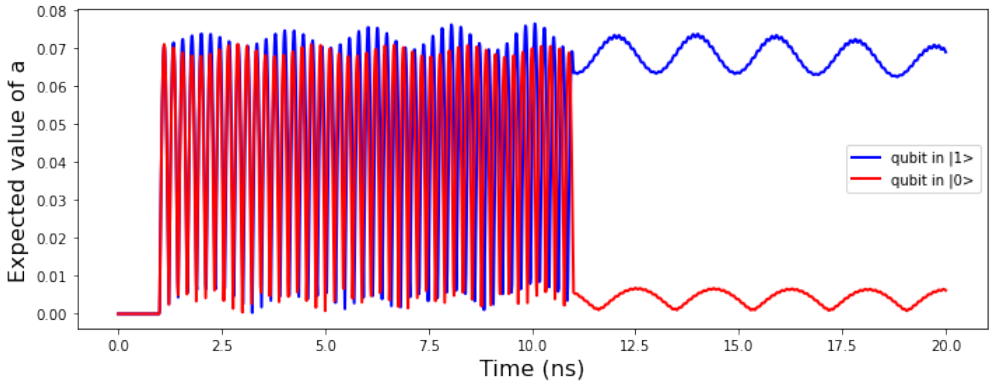

Then we make the discret fourier transform during the interval we applied A and compare the wave frequencies with each qubit state:

```
fig, axes = plt.subplots(1, 1, sharex=True, figsize=(10,4))

axes.plot( np.abs(np.fft.fft(expect(a, res1.states)[200:])), 'b', linewidth=2, label='
axes.plot( np.abs(np.fft.fft(expect(a, res0.states))[200:]), 'r', linewidth=2, label='
#axes.plot(tlist, np.imag(expect(a, res.states)), 'g', linewidth=2, label="cavity")
# axes.set_ylim(0, 1.5)
axes.set_xlim(1200,1400)

axes.set_xlabel("freq", fontsize=16)
axes.set_ylabel("Expected value of a", fontsize=16)
axes.legend()

fig.tight_layout()
```

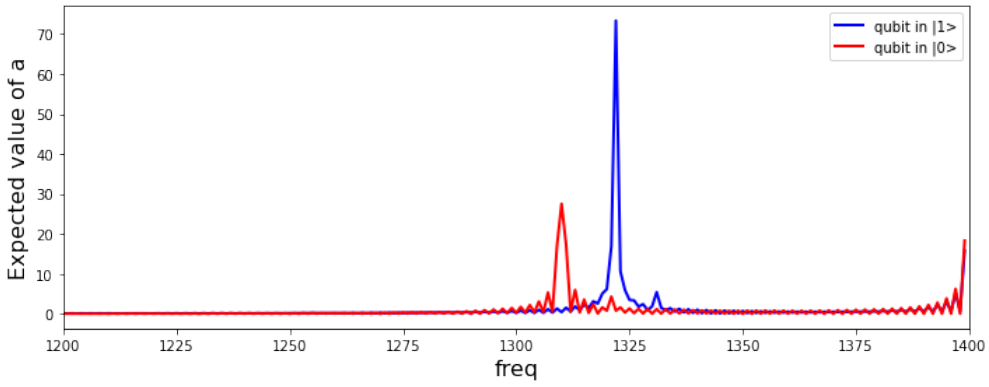

And we notice here how the peak frequency for the qubit in the fourier graph is slightly higher for the qubit in the $|1\rangle$ state than for the qubit in the $|0\rangle$ state like expected. Measuring the qubit would ammount to detecting this difference.

Building quantum chips with Qiskit Metal

Using the tool from IBM, qiskit metal. I studied and modified two notebooks available from IBM tutorials:

- Design a 4 qubit full chip
- Two Crossmons Tunable Coupler

Creating with these two tutorials a notebook for two transmon qubits coupled by a cavity and another notebook for the transmons coupled by a coupler qubit. The first notebook was made by editing the "Design a 4 qubit full chip" tutorial to have only 2 qubits. So some parts where deleted and others rearranged in the code. The second notebook I made to generate the second chip is a mashup of both tutorials. I removed the crossmons which are another type of qubit and added two regular transmons in their place leaving the coupling qubit and rearranging it's position a little. Then using the knowledge of the first tutorial I added the launchpads and the connections between them and the transmons so the qubits can be controlled/measured.

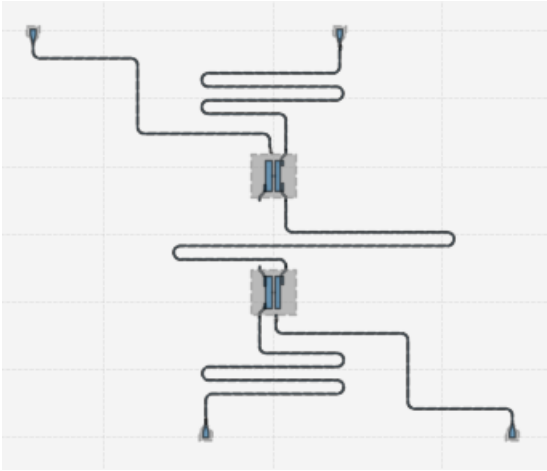

FIGURE 15: Chip of two transmon qubits coupled by a cavity

The qubits coupled by the cavity (chip created in figure 15 and schematic in figure 16). And will change their energy according to the magnetic flux that is generated with a coil over the chip while the cavity doesn't change (figure 17). The qubits can be made to vary with the magnetic flux by having a double Josephson junction both in parallel. When the energy of the qubits is the same as the cavity they enter into a resonance that will allow us to use two qubit gates like the iSWAP. The energy of the qubits depends on many parameters such as the capacitance, the Josephson junction and the resistance in the junction. That way we can tune each qubit to have different behaviors.

The qubits coupled by another qubit (figure 18 schematic in figure 19) have a qubit between them that can have his energy adjusted by the magnetic flux. In that case we can bring the coupler qubit in and out of resonance with either qubit to do the 2 qubit gates like in figure 20. In our chips this might not make a lot of difference. But for multiple qubits this can make it easier to pick the qubits that we want to put into resonance with each other or not put.

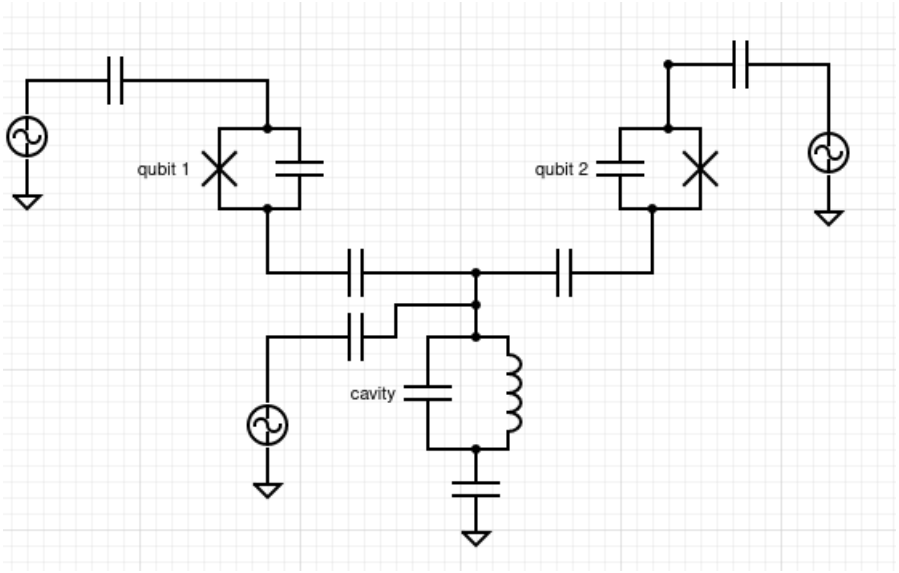

FIGURE 16: Schematic of the chip of two transmon qubits coupled by a cavity

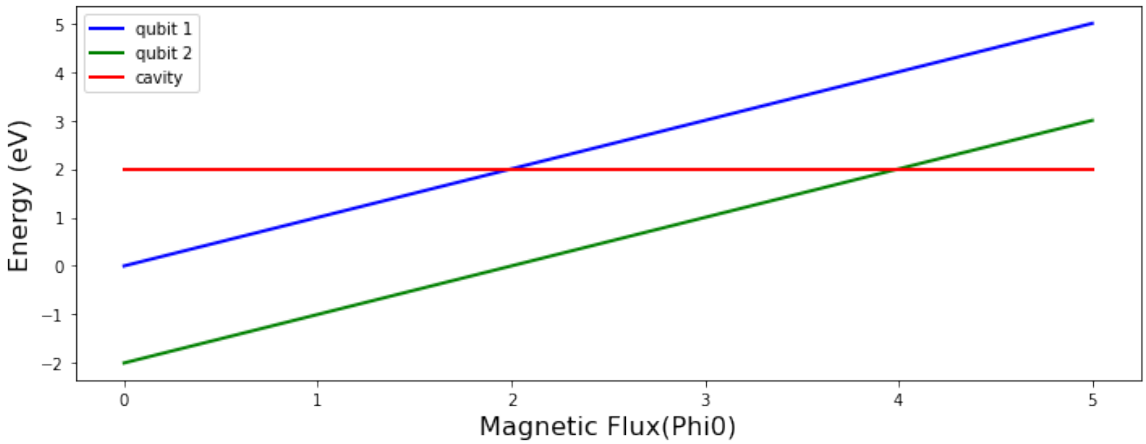

FIGURE 17: Illustrative graph of the energies of the qubits in function of the magnetic flux for two variable qubits and a fixed cavity

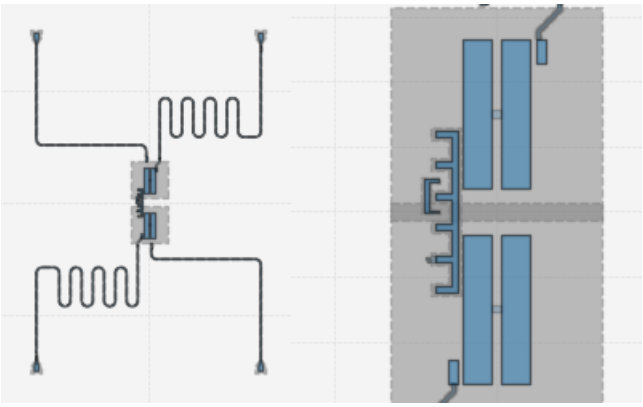

FIGURE 18: Chip of two transmon qubits coupled by a third coupler qubit(with a close up to the right)

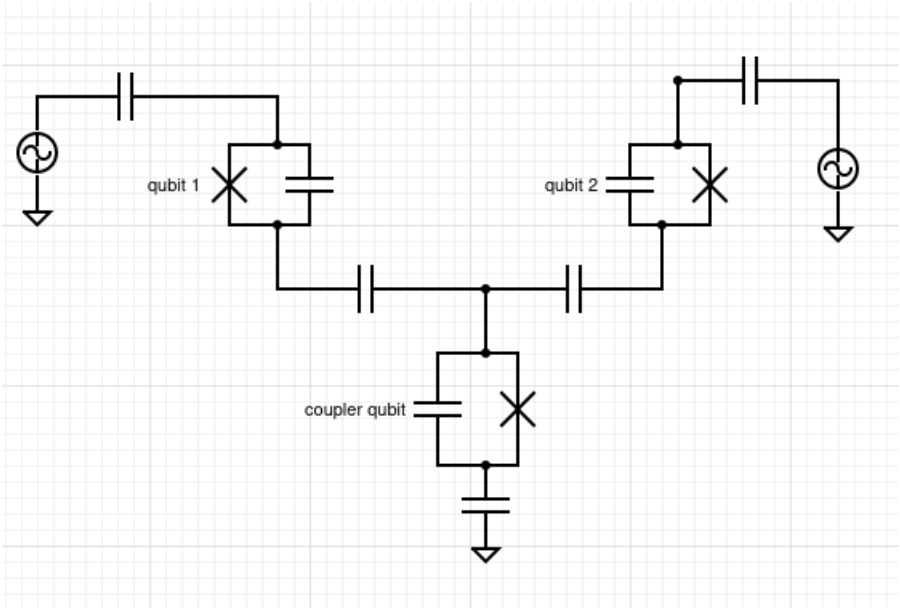

FIGURE 19: Schematic of the chip of two transmon qubits coupled by a third coupler qubit

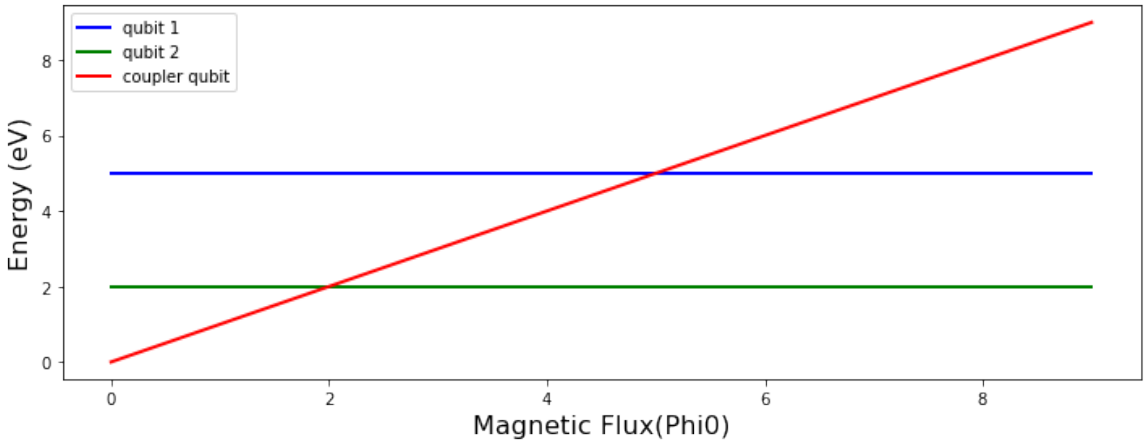

FIGURE 20: Illustrative graph of the energies of the qubits in function of the magnetic flux for two fixed qubits and a third variable coupler qubit

CST electromagnetic simulation of a quantum chip

Here the circuit built in qiskit metal (figure 15) will be simulated in electromagnetic simulators by numerical methods using the Maxwell equations for discreet regions of spaced named meshes. Getting numerical solutions to the electrical and magnetic fields for systems with complex geometries such as this one. The chosen simulator software is **CST** and the circuit used is exported from qiskit metal in the format GDS.

The goal was finding the resonance frequency of the cavity between the two qubits. So it was edited in Klayout to cut out some parts of the circuit and leave only the relevant part in. Then it was imported in CST as a $1\mu m$ thick perfect electro conductor with a subtract of silicon under it (figure 21).

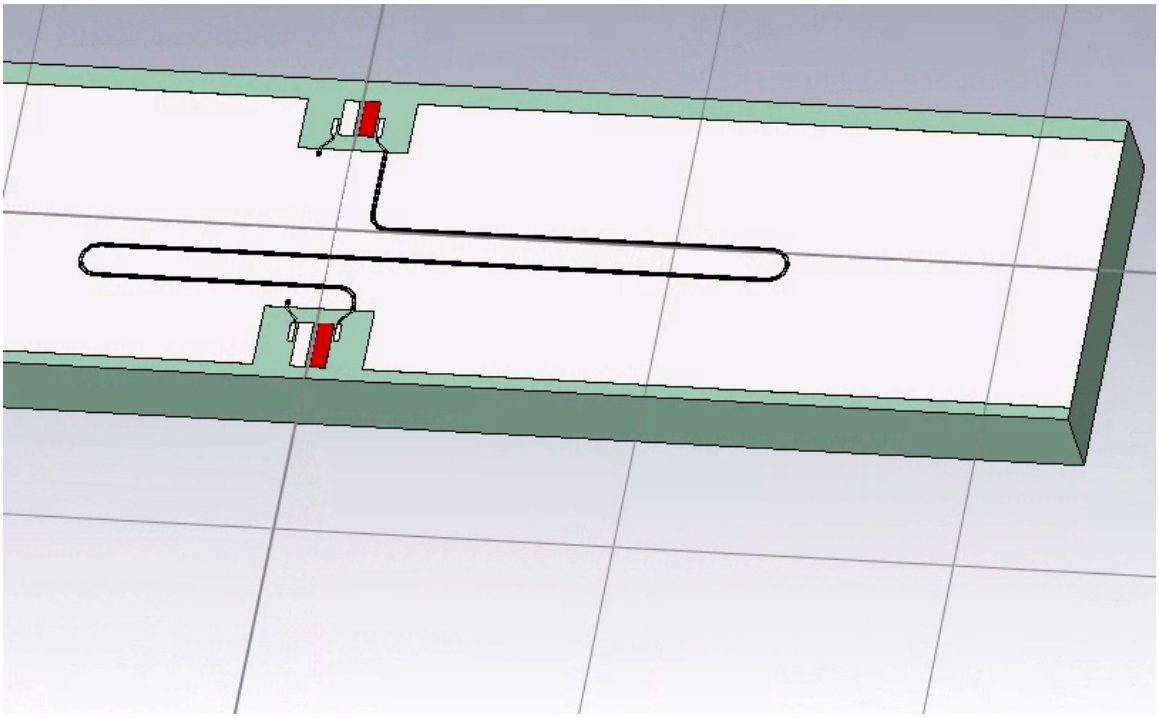

FIGURE 21: 3D model of the circuit for the simulation

The signal input was placed at a plate of one transmon qubit and the output at the plate of the other qubit. And the simulation was run for many frequencies in the interval 0-20GHz. We can see the field monitor for 4GHz, figure 22, and 7Ghz, figure 23.

And finally we can get the resonance frequency by observing the graph of the output of the circuit in the frequency domain (figure 24). We can see the first resonance at around 6.5Ghz and another big one at 7.2-7.5Ghz followed by one at around 11Hz.

The wire of the cavity has 9000μ of length and along with other specifications such as the thickness of the material deposited in the plate the calculated resonance frequency was 6.627GHz using a spreadsheet for circuit design available in the laboratory. Which is not far from the the first small resonance we see in figure 24. This resonance is used in the process of controlling the qubits in the quantum chip bring bringing them either in our out of resonance with the cavity for a iSWAP gate with the cavity for example.

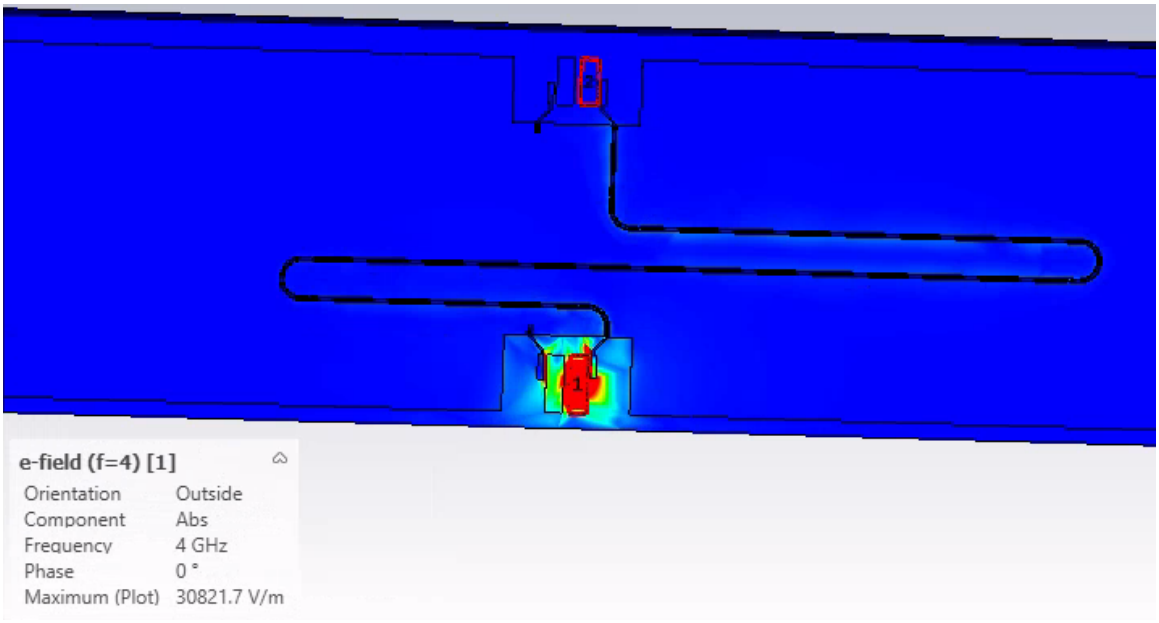

FIGURE 22: Colored graph of the electric field intensity for a input frequency of 4GHz

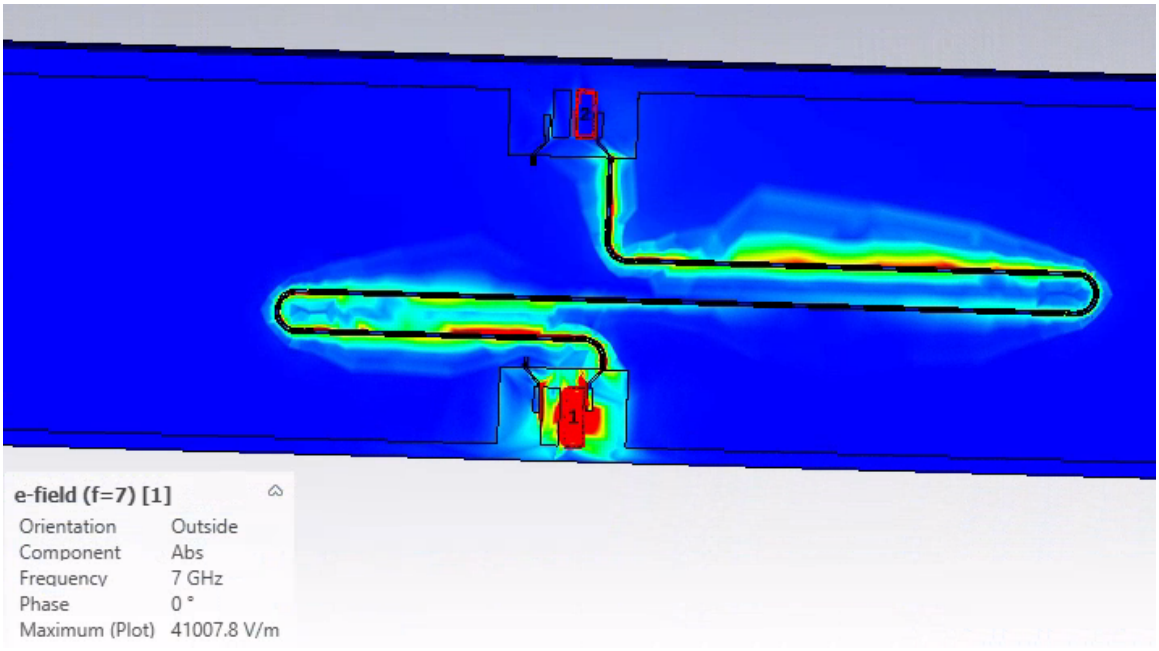

FIGURE 23: Colored graph of the electric field intensity for a input frequency of 7GHz

Conclusion

The beginning of the project was more of a directed study of the basis of superconducting qubit. Going from the properties of the superconductor itself to the Josephson junction and the circuits using it. Here I was able to get a good grasp of the manner in which the superconductor qubits really work from the ground up.

Different from my previous project of scientific initiation where the qubit was assumed

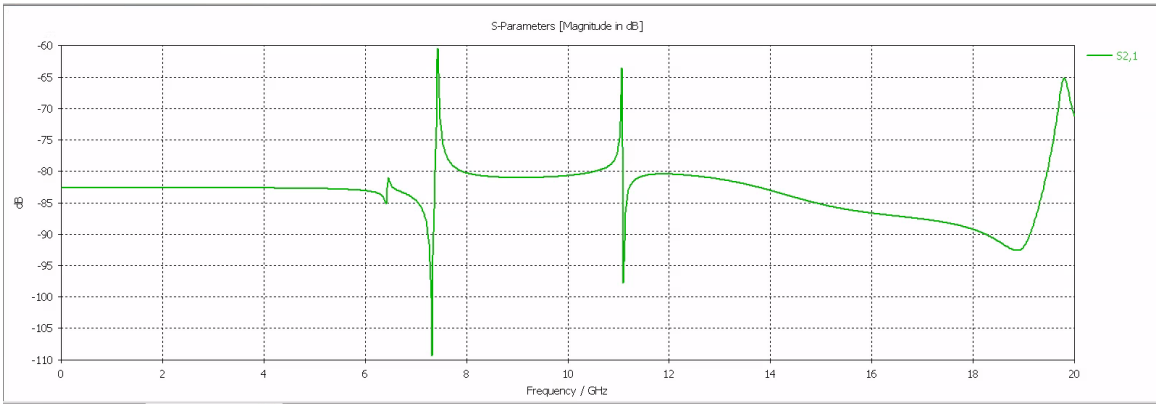

FIGURE 24: Graph in the frequency domain of the amplitude of the signal between the two plates of different transmon qubits connected through a cavity.

to just work. I got to expand basic knowledge of quantum mechanics such as the quantum harmonic oscillator (cavity) with new notions such as non-linearity from the Josephson junction or driven cavities and resonators.

Then in the second part I used this knowledge to build simulations of the quantum circuits using their Hamiltonians. And do some more complex quantum computing operations with them such as a CNOT gate using two coupled qubits. For this part I had to develop better the knowledge of driving qubits with a signal. For which I used a different reference from the used in the beginning [7].

I also simulated the process of calibration of a coupling constant and the simulation of a measurement. This added to the feel of how it would be working with a real superconducting qubit in a laboratory. How it would be controlling it and getting output.

To finish the project I used a new tool by IBM called qiskit metal to design a superconducting chip. And then simulated part of it (the cavity between the qubits) in CST. Which was a bit difficult because CST requires one to know a lot of little tricks for it to work properly which requires experience. But I was still able to get a good simulation with the resonance frequency of the cavity visible.

Following the project I am going now beginning in August on an exchange program to France at Paristech ESPCI to get a double diploma in engineering. Hopefully to also continue my studies in the subject of superconducting quantum computing and get a Masters degree along with the bachelor diploma.

References

[1] F. Arute, K. Arya, R. Babbush, D. Bacon, J. C. Bardin, R. Barends, R. Biswas, S. Boixo, F. G. Brandao, D. A. Buell, B. Burkett, Y. Chen, Z. Chen, B. Chiaro, R. Collins, W. Courtney, A. Dunsworth, E. Farhi, B. Foxen, A. Fowler, C. Gidney, M. Giustina, R. Graff, K. Guerin, S. Habegger, M. P. Harrigan, M. J. Hartmann, A. Ho, M. Hoffmann, T. Huang, T. S. Humble, S. V. Isakov, E. Jeffrey, Z. Jiang, D. Kafri, K. Kechedzhi, J. Kelly, P. V. Klimov, S. Knysh, A. Korotkov, F. Kostritsa, D. Landhuis, M. Lindmark, E. Lucero, D. Lyakh, S. Mandrà, J. R. McClean, M. McEwen, A. Megrant, X. Mi, K. Michielsen, M. Mohseni, J. Mutus, O. Naaman, M. Neeley, C. Neill, M. Y. Niu, E. Ostby, A. Petukhov, J. C. Platt, C. Quintana, E. G. Rieffel, P. Roushan, N. C. Rubin, D. Sank, K. J. Satzinger, V. Smelyanskiy, K. J. Sung, M. D. Trevithick, A. Vainsencher, B. Villalonga, T. White, Z. J. Yao, P. Yeh, A. Zalcman, H. Neven, J. M. Martinis, *Nature* **2019**, *574*, 505–510.

[2] J. Clarke, F. K. Wilhelm, Superconducting quantum bits, **2008**.

[3] R. P. Feynman, *International Journal of Theoretical Physics* **1982**, *21*, 467–488.

[4] S. M. Girvin, R. J. Schoelkopf in, **2015**.

[5] R. Gross, A. Marx, F. Deppe, *Applied Superconductivity: Josephson Effect and Superconducting Electronics*, Walter De Gruyter Incorporated, **2016**.

[6] H. L. Huang, D. Wu, D. Fan, X. Zhu, Superconducting quantum computing: a review, **2020**.

[7] P. Krantz, M. Kjaergaard, F. Yan, T. P. Orlando, S. Gustavsson, W. D. Oliver, *Applied Physics Reviews* **2019**, *6*, 021318.

[8] M. A. Nielsen, I. L. Chuang, *Quantum Computation and Quantum Information*, 10th anniv, Cambridge University Press, Cambridge ; New York, **2010**, p. 676.

[9] G. Wolfowicz, J. J. Morton in *eMagRes*, *Vol. 5*, 4, John Wiley & Sons, Ltd, Chichester, UK, **2016**, pp. 1515–1528.